Developing a novel filter material for protective gears for health care (COVID -19) from BCTMP (Bleached Chemi-Thermo-Mechanical Pulp)

by

Ziyi Lin

A thesis submitted in partial fulfillment of the requirements for the degree of

Master of Science

in

Chemical Engineering

Department of Chemical and Materials Engineering
University of Alberta

Abstract

Under the background of COVID-19 global pandemic, personal protective equipment (PPE), especially masks, has been highly demanded. Also, this high requirement has resulted in ocean pollution since the main material, polypropylene, is non-biodegradable and expensive. The producing processes are also complicated. To solve the scarcity of PPE and the environmental risks caused by commercial masks, people have been concerned to use environmentally friendly and inexpensive materials. Wood-pulp-based filter media have been studied for years. This thesis developed a novel filter material bleached chemi-thermo-mechanical pulp. Filter papers were made from two grades of wood pulp separately. Basis weight of them was half of that of the N95 mask middle layer (filter layer). Morphology of pulp filters was analysed by digital and scanning electron microscope (SEM). Filtration efficiency and pressure drop of pulp filters were measured and compared with commercial N95 masks. To simulate ultra-fine particles, activated carbon powder and candle smoke were used. Both traditional N95 masks and novel filter media showed satisfying performance on carbon powder collection, while pulp filters performed better on candle smoke tests. The only problem for pulp filters is the high pressure drop, which reflects the breathing resistance. Hence, from the filtration efficiency side, wood pulp has the potential to be a raw material of masks. However, the high pressure drop as well as filters with basis weight close to middle layer of N95 masks need further studies.

Preface

This thesis is an original work by Ziyi Lin. No part of this thesis has been previously published.

Acknowledgements

This thesis summarizes the work I have conducted during the two beautiful and colorful years at the University of Alberta. The little contribution to the potential use of wood pulp in high efficiency particle filters would not be possible without the support of my supervisors, Dr. Rajender Gupta and Dr. Wei Victor Liu, research mentors, families, and friends.

I would like to express my gratitude to Dr. Rajender Gupta and Dr. Wei Victor Liu for their guidance and encouragement throughout the program. Their mentorship has been extremely helpful in shaping and improving my capabilities to being an independent researcher. Their supervision has helped me a lot in exploring a new field in different dimensions. I also acknowledge Mr. Ron Erickson from Millar Western Forest Products Ltd., who has provided wood pulp samples and pulp filter sheet samples during the program. Their suggestions and comments are innovative, valuable, and motivating during my project.

I am also grateful to Dr. Md Khan for offering constant help on experiments. I would also be thankful to all members in Dr. Gupta's group for their cooperation in laboratories.

I would also appreciate the help and assistance of Dr. Guibin Ma in conducting the SEM and EDX tests. I also thank all professors and staff members at the University of Alberta for all information and assistance during my study.

Finally, I would also like to be grateful to my beloved families for their constant support and encouragement. And my friends at university and those back home, Xinwei Lyu and Zeming Song. Thank you all for your support and love.

Table of Contents

List of Tables

List of Figures

Chapter 1

Introduction

1.1 Background

Under the background of COVID – 19 pandemics, the personal protective equipment (PPE) is essential for both healthcare workers and the general people to lower the possibility to be infected and limit the spread of coronavirus. Wearing a mask or face covering is suggested by World Health Organization guideline. This results in a scarcity of face masks and other personal protective gears all over the world. However, it is not a big problem since it can easily be solved by producing more. During the pandemic, many companies have volunteered to produce healthcare equipment, such as surgical masks, hand sanitizer. The most serious challenge is the efficiency of the face masks on filtering coronavirus, in other words, ultra-fine particles, distributing in liquid droplets or aerosols. It has been proved that the commonly used medical face masks only provide protection to some specific extent, such as when combining with social distancing. This is because the surgical mask only performs as a barrier between the wearer and other people by changing the exhaled airflow distribution. Physically the surgical masks or simple mouth-and-nose covers convert the jet like airflow with high exit velocity from the mouth to an indirect air movement with low velocity coming outside the mask [1]. Consequently, wearing a mask during normal face-to-face conversation may be helpful to limit the transition of infectious viruses via aerosols. This has also been proved by previous reports during SARS outbreak [2]. However, the surgical mask does not work sufficiently in highly contaminated environment, specifically in hospitals. This is because it

can only restrain large particles, while the ability of capturing sub-micro particles is limited. Therefore, it may not provide complete protection from germs or other contaminates, let alone the improper use, such as loose fitting. Only N95 respirators have the ability to block fine particles down to 0.3 μm with a at least 95% efficiency, if properly used.

Besides the low filtration efficiency of medical masks, materials and the processes of producing them contribute to the fact that surgical masks are not the most proper equipment during the pandemic. Surgical as well as N95 masks are usually made of polypropylene using spun-bond and melt-blown technology [3], which are not only time consuming but also cumbersome to set up. Given the inconvenience of producing processes and the low filtration efficiency on ultra-fine particles, some studies have been focusing on using novel materials to improve masks' performance.

Another problem that masks facing is raising environmental pollution risks. The raw materials of masks are plastic polymers, especially polypropylene. These materials are highly liquid-resistant and non-biodegradable and may carry infectious viruses [4]. The only method to treat them is the landfill and the polymer ends up as microplastic and/or nanofiber contaminants in the literring and water system [5]. The existence of ultra-fine plastics in the aquatic environment is easy to be mistaken as food and eaten by marine animals and may affect the food chain and marine ecosystem eventually [4]. Since the enormous usage of masks, this risk will extend to the future and continuously do harm to marine life. It is estimated that approximately 0.15 million tons to 0.39 million tons of plastic debris will end up in global ocean within a year [6]. And this is more severe in low-income countries because of the lack of waste treatment facilities.

Concerning the air quality and environment people are in as well as the scarcity of PPE, some researchers are trying to extract contaminates from used masks so that masks can be used multiple times. Another method is to produce more healthcare gears with environmentally friendly, biodegradable and inexpensive materials. Many researchers have claimed that wood pulp has the potential to be raw materials of high efficient filters.

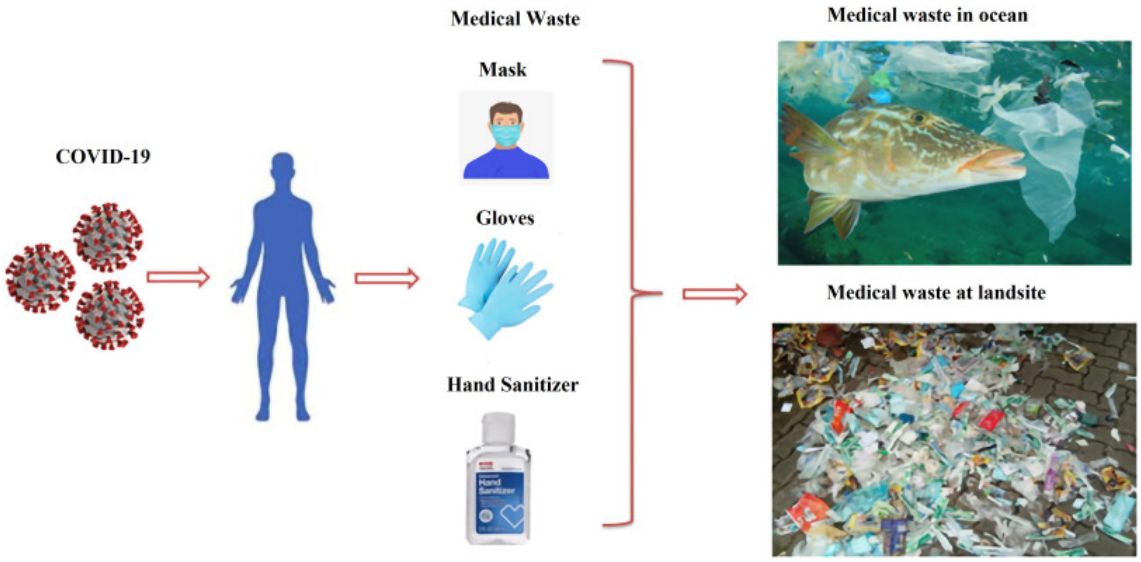

Figure 1.1: Plastic waste in the ocean [7]

1.2 Literature Review

1.2.1 Standard N95 masks and filtration testing procedures

Commercial N95 masks

NIOSH certifies the N95-class filters for Not-resistant to oil series with a filtration efficiency no less than 95% [8]. Besides collection efficiency, pressure drop, which reflects breathing resistance, is another important factor to determine filtration performance. The initial inhalation and excalation resistance should not exceed $35mmH_2O$ $(343Pa)$ and $25mmH_2O$ $(245Pa)$, respectively [9].

Standard N95 masks mainly consist of polypropylene (PP) fibers spun by different technologies, such as spun-bound and electrostatic non-woven technology [10]. The middle layer, the filter layer, is made of polyester/cellulose. The filtration layer is also filled with metal ions, which create an ionic field, to improve the filtration efficiency without increasing breathing resistance [11].

Filtration performance testing

According to NIOSH [12] testing procedures, filters should be challenged by a NaCl aerosol at 25 ± 5^oC and a relative humidity of $30 \pm 10\%$. The aerosol should be neutralized to the Boltzmann equilibrium state before passing through tested filters. The particles have a size distribution with a count median diameter of $0.075 \pm$

0.020 μm and a geometric standard deviation not exceeding 1.86. The aerosol concentration applied to each unit of filters should not exceed 200 mg/m^3. Filters should be tested at a flow rate of 85 L/min. Based on the surface of standard N95 masks that the wearer would breathe, the face velocity can be calculated by dividing the flow rate against effective area [13]. The determined area is approximate 175 cm^2, thus the face velocity is 8.1 cm/s [14]. Considering different wearing situations, Huang et al. [15] used face velocities at $4, 8$, and 12 cm/s for light, moderate, and heavy workloads, respectively.

1.2.2 Depth filters

The commonly used medical masks or high efficiency respirators, such as N95 respirators, contain at least three layers, which produce a filtration system or a depth filter. Each layer in this system has different properties, working processes and filtration mechanisms.

These three layers are always thermal-bond layer, staple fibers, and melt-blown layer from the outer to the inner layer [16]. The sequence of layers are based on their properties, which provide them different functions. The outer layer is always the lightest and has the largest pore size, while the middle and inner layers are heavier and have smaller pore size. Thus, the particles or aerosols or suspension will experience a decreasing pore size during filtration [16]. Since the first layer is more porous, the function of it is to collect large particles and reduce particles loading on the surface of the filter system. Besides, the thermal-bond layer has lower melting point, therefore, it can stiffen the filter media, especially when the operating pressure decreases. The second layer, the staple fibers, is used to capture large number of particles due to the inner connected pores and torture paths. The final layer, the melt-blown layer, exhibits the lowest porosity and smallest fiber diameter, therefore, the function of it is to collect ultra-fine particles in high efficiency [17]. Normally a depth filter has four filtration processes, namely surface straining, depth straining, depth filtration and cake filtration [18].

1.2.3 Mechanisms of depth filters

There are five commonly believed mechanisms, namely size exclusion, inertial impaction, interception, diffusion and electrostatic attraction [19] [20] [21]. Different mechanisms work for different size ranges of particles. Size exclusion mainly works for large particle filtration. Surface restraining and depth filtration are based on this mechanism. Inertial impaction works for particles with diameter larger than 1 μm.

Interception is for particles with diameter ranging from 0.1 to 1 μm. Diffusion is one of the most important mechanisms for depth filter. It only works for small particles (smaller than 0.1 μm). The last mechanism, electrostatic attraction, is another important mechanism. It can be applied to collect ultra-fine particles with diameter in the range of 0.15 to 0.5 μm, which is difficult for other mechanisms. Fig. 1.2 shows three of filtration mechanisms and the efficiency of them [22].

Inertial impaction

This mechanism happens when the particles are too large to change their route following the airstream, due to inertia. They continue their original path and finally hit and stick to the filter fibers. (see Fig.1.2a)

Interception

Interception occurs when the particles are close enough to the fiber surface, usually within particle diameter. Then the particles will be captured by the fiber surface. (see Fig. 1.2b)

Diffusion

Diffusion applies to particles that are small enough comparing to the space around them. Therefore, there are enough space to zigzag around before being attracted to filter fibers. (see Fig. 1.2c)

Electrostatic attraction

Electrostatic force between fibers and particles plays a significant role in the filtration process. It has been applied to various HEPA filters (high efficiency particle air filters), such as N95 respirators. PAE (Polyamide-amine-epichlorohydrin) has been used to provide positive charges to fiber surface [23]. This can be achieved by charging particles or fibers or applying externally electric field.

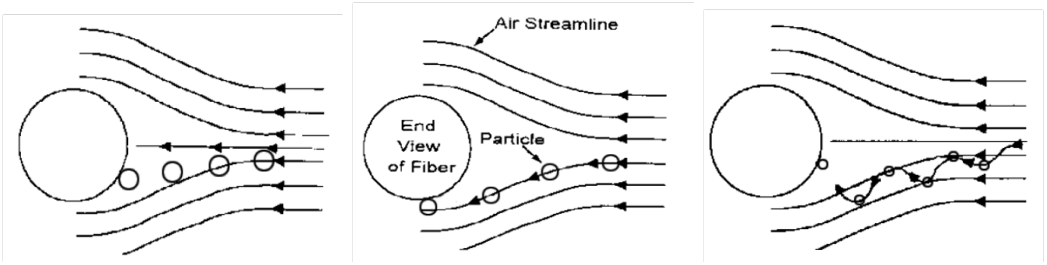

(a) *Inertial impaction* (b) *Interception* (c) *Diffusion*

Figure 1.2: Filtration mechanisms [22, 24]

1.2.4 Filtration processes

Different size ranges of particles have different filtration mechanisms, similarly, the filtration processes of them are also different. The filtration process is also related to particle concentration deposited on the filter. At the beginning, particles are more likely to be captured by fiber surface. As time goes, particles are collected by other particles that have already stuck on the fiber surface. Particle dendrites are formed. In addition, smaller particles, because of low Stoke number, still follow the air streamline, penetrate through the dendrite structure, and go deep inside of the fibrous filter [25]. Finally, there is a particle cake forming on the surface of the fibrous filter. The particle cake also acts as a filter medium and block particles. These three processes are called depth filtration, cake formation and cake filtration, respectively. Fig.1.3a shows the modelling of filtration processes with dimensionless time with a fiber diameter of 15 μm and an SVF (Solid Volume Fraction) of 19% [26]. For dual filters, an internal cake will form between two layers. Fig. 1.3b models this process [27].

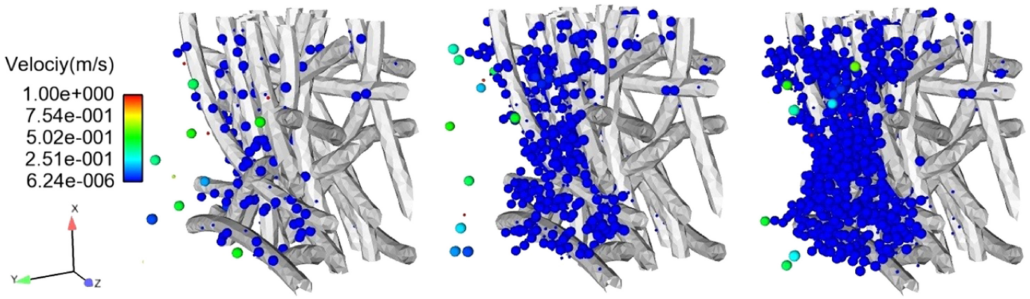

(a) *Filtration process models with dimensionless time for a fibrous filter with fiber diameter of* 15 μm *and a SVF of* 19%

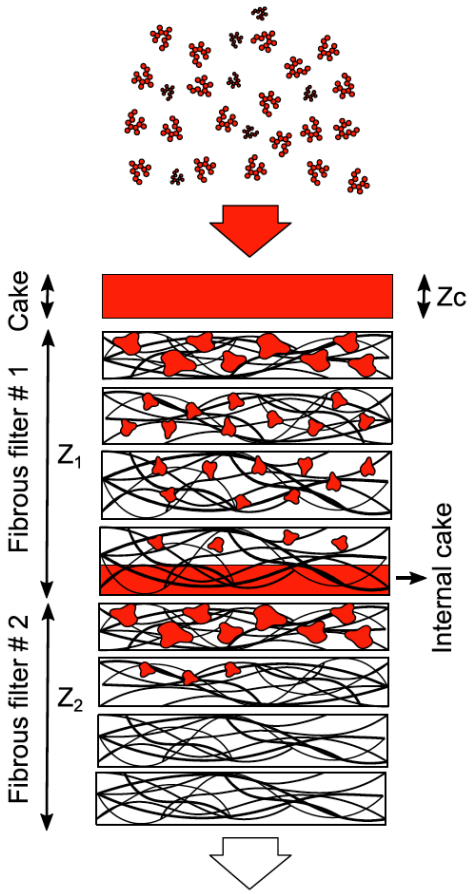

(b) *Filtration model of a dual filter*

Figure 1.3: Filtration process models [26, 27]

1.2.5 Parameters affecting filtration performance

Performance of depth filters is directly related to two properties, pressure drop and filtration efficiency. Better filtration performance requires a relatively low pressure drop and a relatively high filtration efficiency. Large pressure drop makes it difficult to breathe and consumes more energy when using in building ventilation systems.

To easily express the relation between these two properties, a new parameter, filter quality(QF), has been introduced [28] (see eq. 1.1 & 1.2).

$$QF = -\frac{(1-E)}{\Delta P} \tag{1.1}$$

$$E = \left(\frac{C_u - C_d}{C_u}\right) * 100\% \tag{1.2}$$

, where E represents collection efficiency, ΔP is pressure drop, C_u, C_d are concentration of upstream and downstream, respectively.

Theoretical pressure drop evaluation

The pressure drop of fibrous filters can be separated into two processes: initial pressure drop, which is the air resistance of a clean filter, and the pressure drop of the filter deposited with particles. During different filtration processes and mechanisms, the estimation methods are different. Davies [29] provided a mathematical prediction of clean filters (see eq. 1.3). Bergam [30] took particle size into consideration and modified Davies's model (see eq. 1.4), when it comes to filters deposited with particles. The pressure drop of a loaded filter also can be regarded as the pressure drop both a clean filter and the deposit. Thomas et al. [27] developed a new model based on this. The theoretical equations of initial pressure drop (eq. 1.3) and filters loaded with particles (see eq. 1.4 and eq. 1.5) are shown below:

$$\frac{\Delta P}{Z} = 64\mu\ U_0 \frac{\alpha^{3/2}(1+56\alpha^3)}{d_f^2} \tag{1.3}$$

, where ΔP is the pressure difference between the upstream and downstream of the clean filter (Pa), Z is the total fiber thickness (m), μ is the gas dynamic viscosity, U_0 is face velocity (m/s), α is the packing density, which is defined by the ratio of volume of fibers to the total fiber volume, d_f is the mean equivalent filter diameter (m) [31].

$$\Delta P = 64\mu\ U_0 Z \left(\frac{\alpha}{d_f^2} + \frac{\alpha_p}{d_p^2}\right)^{1/2} \left(\frac{\alpha}{d_f} + \frac{\alpha_p}{d_p}\right) \tag{1.4}$$

, where d_p is the particle diameter, α_p represents the particle volume fraction.

$$\Delta P = \frac{\Delta P_0 \left(\frac{\alpha_f}{\alpha_f + \frac{\alpha_p}{\alpha_d}} \right)^{1/2} + \Delta P_d \left(\frac{\frac{\alpha_p}{\alpha_d}}{\alpha_f + \frac{\alpha_p}{\alpha_d}} \right)^{1/2}}{1 - \alpha_f - \alpha_p} \tag{1.5}$$

, where α_f represents fiber packing density, α_p represents particle packing density (volume of collected particles/volume of fibrous filter), α_d represents deposit density (volume of collected particles/volume if the deposit), ΔP_0 is the initial pressure drop, which can be predicted from Davies' equation (eq. 1.3). ΔP_d is the pressure drop of deposit [27] (see eq. 1.6)

$$\Delta P_d = 64 \frac{{\alpha_p}^{1/2}(1 + 56\alpha_p^3)}{d_{pp}^2 C u_{pp}} \mu Z U_f \tag{1.6}$$

, where d_{pp} is the primary particle diameter, Cu_{pp} is the slip correction factor (calculated with d_{pp}), α_d is depositing packing density, which can be calculated from the equation below [see eq. 1.7]. In this expression, Pe is the Peclet number, which is a function of count median diameter of particle size distribution [27] .

$$\alpha_d = 1 - \frac{1 + 0.438Pe}{1.019 + 0.464Pe} \tag{1.7}$$

$$Pe = \frac{CMD * U_f}{D} \tag{1.8}$$

, where CMD is the count median diameter (m), D is the diffusion coefficient (m^2/s).

However, Bergan's model did not consider cake filtration and surface filtration processes. When the filter is getting almost saturated, a filtration cake will form on the filter surface, which contributes to an increase in the pressure drop and collection efficiency. The pressure drop of the cake has a different prediction model [27] (see eq. 1.9)

$$\Delta P_G = 64 F_c \frac{{\alpha_d}^{3/2}}{d_{pp}^2 C u_{pp}} \mu Z_c U_f \tag{1.9}$$

,where Z_c is the cake thickness, F_c is the correction factor and equals to 1.5.

Theoretical collection efficiency prediction

Based on filtration mechanisms, the total collection efficiency ($E_{\Sigma,n}$) is related to single fiber efficiency due to mechanical force (E_m) and electrical force ($E_{e,n}$). For air-cleaning equipment, penetration of a particle with n elementary charges (P_n) is more commonly used. It is the ratio of number or mass concentration that entering and exiting the filter [32].

$$E_{\Sigma,n} = 1 - (1 - E_m)(1 - E_{e,n}) \tag{1.10}$$

$$P_n = exp\left[\frac{-4\alpha\chi E_{\Sigma,n}}{\pi d_f(1-\alpha)}\right] \tag{1.11}$$

By assuming all mechanisms work independently and particles are at Boltzmann charge equilibrium, Hinds [32] gave the relationship between total collection efficiency and efficiency of each mechanism, see eq.(1.12).

$$E_{\Sigma,n} = 1 - (1 - E_r)(1 - E_d)(1 - E_{dr})(1 - E_i)(1 - E_g) \tag{1.12}$$

$$E_{\Sigma,n} \approx E_r + E_i + E_d + E_{dr} + E_g \tag{1.13}$$

,where E_r represents the single fiber efficiency for interception[33], E_i is that for impaction[34], E_d is that due to diffusion[29, 33], E_{DR} is the efficiency due to interception and diffusion [35], E_g is for gravitational settling [32]. Thus, this may overestimate the efficiency, because different mechanisms are competing for the same particle and its capture could be counted twice [32].

Fig. 1.4 shows the collection efficiency against particle diameters for different mechanisms and total efficiency. The most penetrating particle size (MMPS), which is about $0.3\mu m$ is also shown in the figure.

Factors affecting pressure drop and filtration efficiency

Pressure drop and collection efficiency are the most direct factors qualifying a high filtration efficiency filter. Pressure drop reflects the air resistance or breathing re-

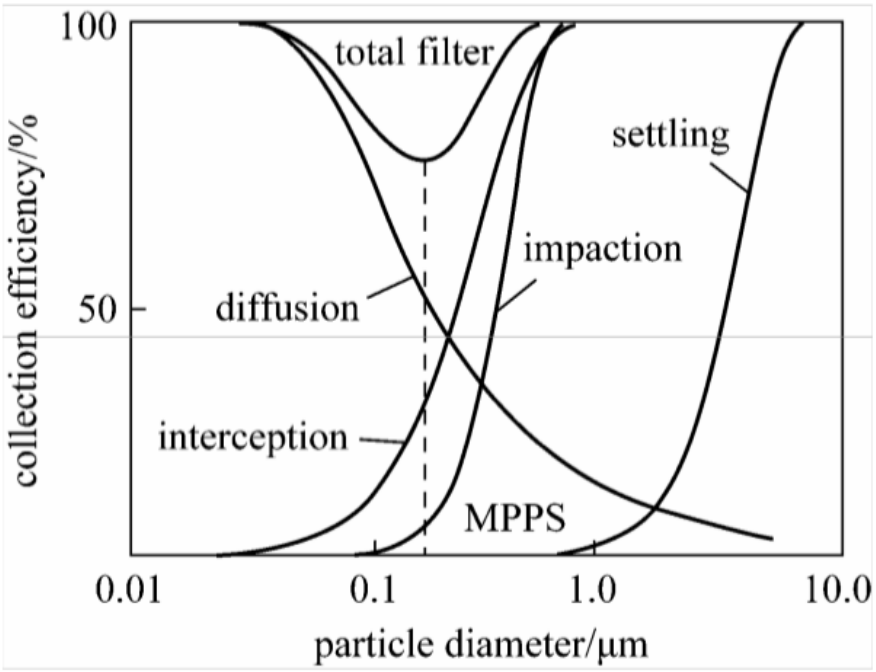

Figure 1.4: Collection efficiency for single-fiber of particles with different diameters and total efficiency [36]

sistance of the filter media. Lower resistance consumes less energy in ventilation systems, and similarly people will find it more comfortable to wear.

There are some physical characteristics affecting pressure drop and collection efficiency, such as particle size distribution, filter porosity, fiber diameter, filter geometry and thickness of the filter media. And operating conditions can also change filter media performance.

Particle size

According to NIOSH standard test conditions [8], the count median diameter should be $0.075 \pm 0.02\mu m$ with the geometric standard deviation smaller than 1.86. And the aerosol concentration should not exceed $200mg/m^3$.The loading target is $200 \pm 5mg$. Besides NIOSH standards, another essential parameter is the most penetrating aerosol size (MPPS) for mechanical filters. The most penetrating particles size is the size of particles that are most likely to penetrate into filter media. It is commonly believed to be $0.3\mu m$ [8]. However, many studies have shown that it depends on operating conditions, filter medium, particle's shape and charge [37]. Therefore, the MPPS can be expressed as the range of 100 to $300\mu m$ [37].

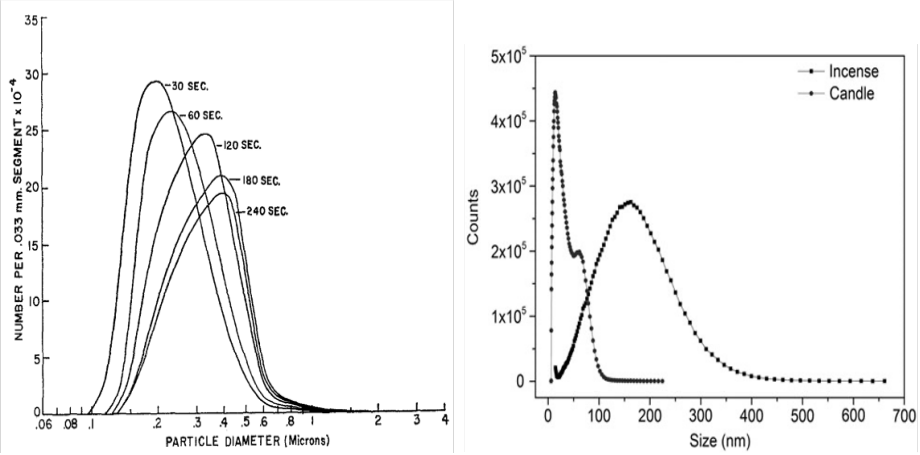

(a) The effect of aging on diluted cigarette smoke

(b) Candle and incense smoke. The y values are in arbitrary units

Figure 1.5: Particle size distribution of cigarette, candle and incense stick smoke [38, 39]

Besides NaCl aerosol used by NIOSH, there are other particles in nano-size, such as the smoke of cigarette, candles, incense sticks and anti-mosquito products. The carbon emitted by burning candle, incense stick or anti-mosquito products has the diameter of 35, 160 and 140 nm, respectively [40]. NE Klepeis et al. [41] believe that the side-stream smoke of cigarette is roughly 200 nm, while cigarette smoke size distribution is also related to time. C.H. Keith et al. [38] proved that particles tend to coagulate over time to form relatively bigger particles, as shown in Fig. 1.5a. However, candle smoke is more complicated. Some studies claim that it has a peak diameter of 11 nm firstly, the particles coagulate to form relatively bigger particles of 27 nm. After about 30 minutes, much bigger particles, with a diameter of 60 nm and above are formed. Correspondingly, the number of particles at smaller diameters decrease [39]. There are some other researchers believing that particle size distribution is linked to burning situations, complete and incomplete combustion. Candles have different burning modes, including steady burning, sooting burning and smouldering mode. Particle size distribution in each burning mode is different. Steady burning only produces ultra-fine particles with the diameter approximate 25 nm, whereas sooting mode particles have the geometric mean diameter of 270 ± 30 nm. The maximum diameter (335 ± 30 nm) of particles were emitted from the smouldering mode [42].

Filter porosity

More porous media exhibit higher air permeability, in other words, lower pressure drops, which leads to higher filter quality value, especially at the initial stage, however, this improvement does not show many advantages over time [43].

Fiber diameter

As fiber diameter reduces, aerosol penetration rate decreases, this can be explained by the fact that thinner fibers contribute to larger surface areas, so that there are more spaces for particles or aerosols to deposit, and for electret fibers, more charges can be carried. This is also the reason the bottom layer in the depth filter has the thinnest fiber. However, when it comes to filter performance, pressure drop must be taken into consideration. For the same area of filter media, thinner fibers result in high packing density, which contributes the increase in air resistance. The influence is more significant than that in filtration efficiency. However, for large particles (> 1 μm), the mechanism interception dominates the whole process, where the collection efficiency is proportional to the ratio of particle diameter to fiber diameter [44].

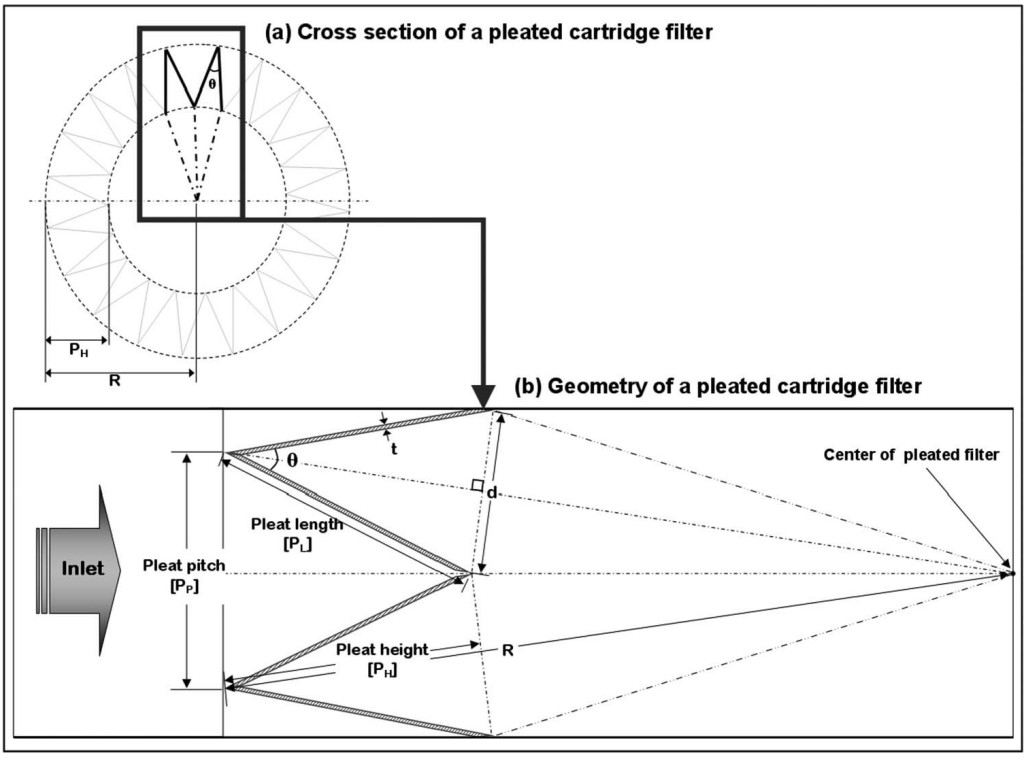

Figure 1.6: Geometry of a pleated filter [45]

Filter geometry

The geometry also plays an important role in affecting filtration efficiency. Pleated filters have been widely used in industry. This is because for filters with the same dimensions, pleated filters have more active filtration area, so that the lifetime of the depth filter can be prolonged [45]. To easily study the geometry of filters, a dimensionless parameter, α, has been introduced. It is a function of pleat height (P_H) and pleat pitch (P_P), and the optimum option of the index (α) is 1.48 [45].

$$\alpha = \frac{P_H}{P_P} = \frac{P_L cos\left(\frac{\theta}{2}\right)}{2\pi R/N} \tag{1.14}$$

, where t P_H, P_P, P_L, θ, and R have been shown in Fig. 1.6, N is the number of pleats.

Thickness

Higher thickness increases the depth of filters, which prolong the time particles passing through filter media. Thus, particles are more likely to be captured by filter fibers. However, thicker filters increase resistance at the same time. This may may consume more energy for building ventilation system and make it more difficult to breathe for personal protective equipment. It has been proved that thickness can promote the filtration efficiency, but has few effect to filter quality [44] (shown in Fig. 1.8b).

Face velocity

Face velocity is also responsible for filtration quality. Lower flow rate is recommended, this is because for aerosol particles in size range $< 1\ \mu m$, the dominant mechanisms are diffusion and electrostatic attraction [44]. Lower face velocity provides lower inertia and longer retention time so that bridges between particles can form. In contrast, higher flow rate results in higher dragging force, therefore, the particles tend to penetrate deep into channels and also increase the pressure drop [43]. Normal nostril breathing can be regarded as a sinusoidal profile [46] shown in Fig. 1.7. The highest breathing velocity reaches 5 m/s, which is much higher than

texting velocities.

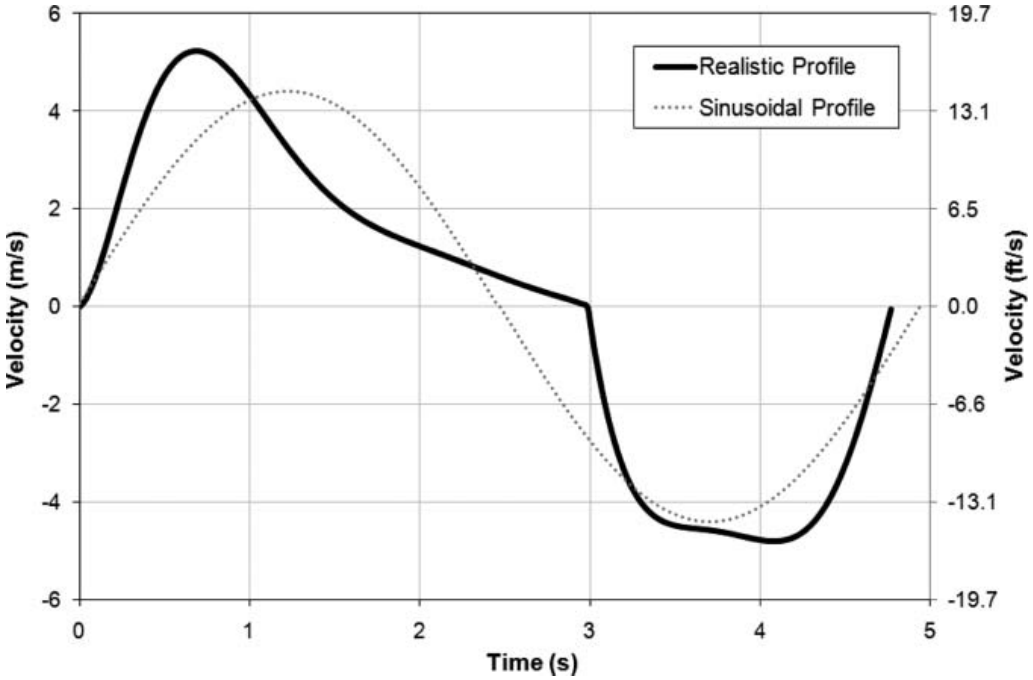

Figure 1.7: Sinusoidal and realistic breathing profiles [46]

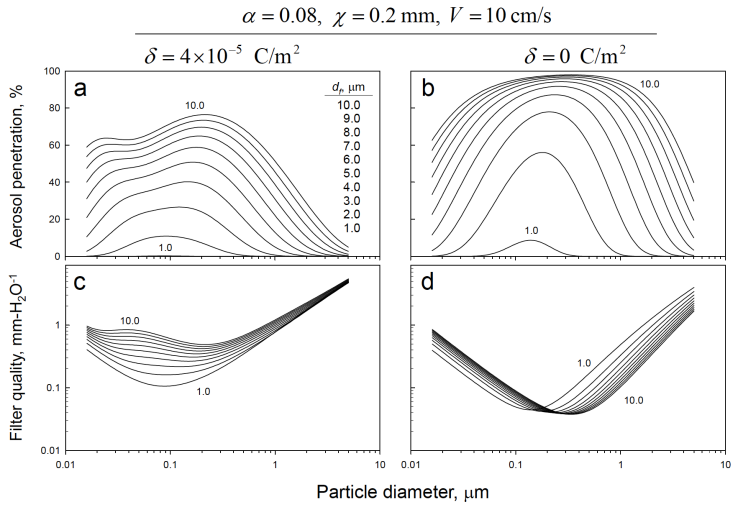

(a) Fiber diameter

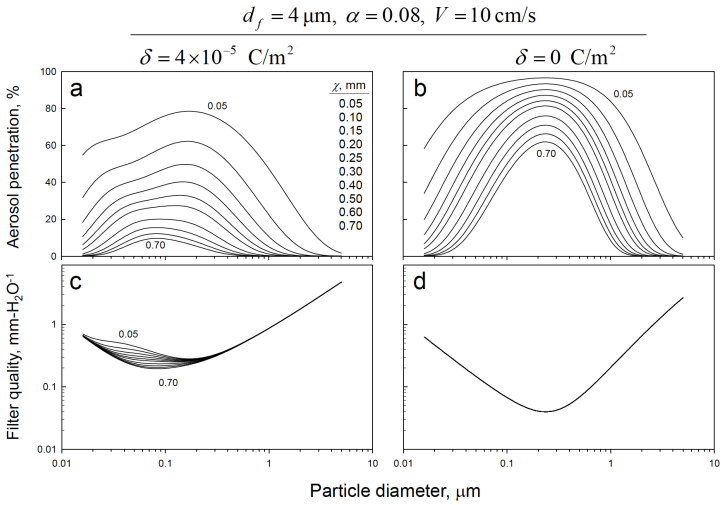

(b) Thickness

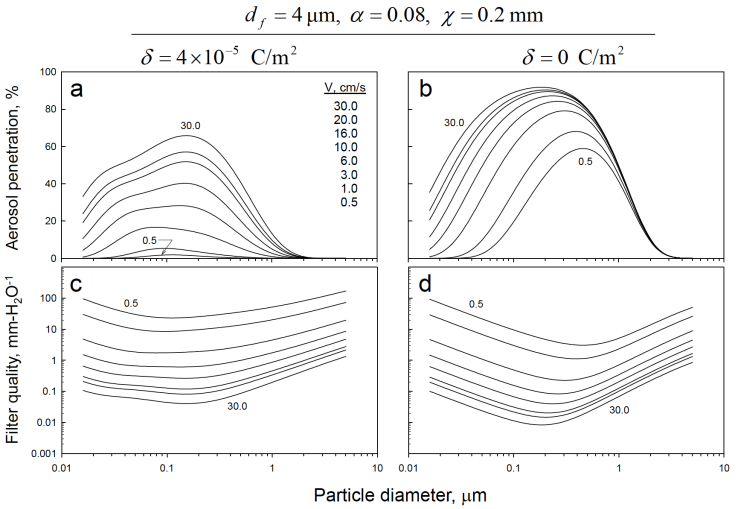

(c) Face velocity

Figure 1.8: Factors affecting filtration efficiency and filter quality for both charged and uncharged filters, where d_f is particle size, α is packing density, V is face velocity, δ is fiber charge density, χ is filter media thickness [44]

1.2.6 Methods of improving filtration performance

During a long time, people have been working on promoting the filtration performance. There have been three widely used methods: the addition of separators or filter aids or nano-fibers. Considering the global pandemic, to slow the spread of infectious viruses, a bacterial-destroying material has also been added into filter media [47].

The addition of separators

Separators can contribute to the uniform distribution of flow or aerosol between layers (as shown in Fig. 1.9), which can effectively avoid local saturation [18]. This is because the well-distributed flows or aerosols increase the possibility to follow through the entire medium. In this case, the separators are usually put between layers or on the top of the first layer.

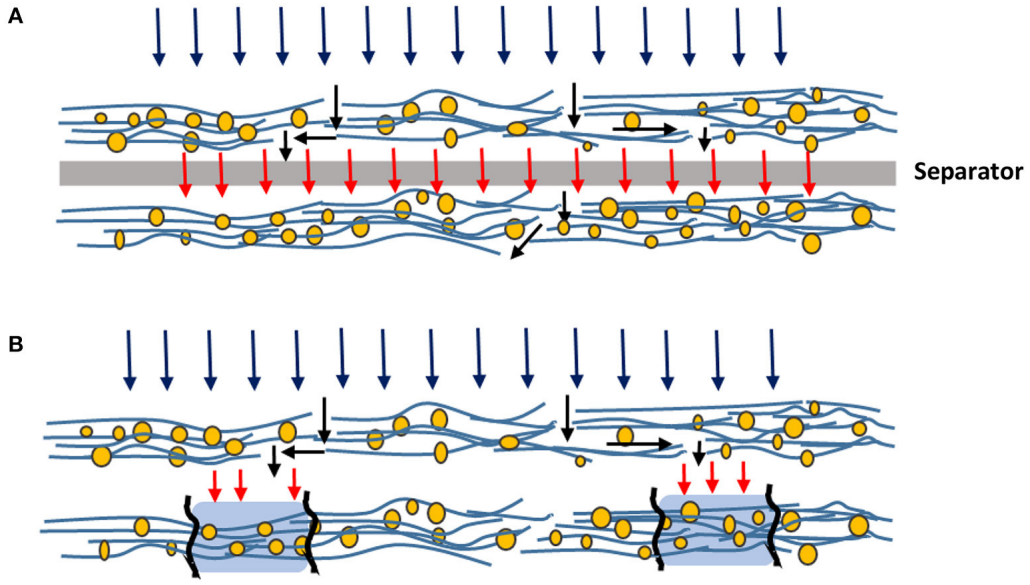

Figure 1.9: Schematic illustration of flow through filter with (A) and without (B) a separator [48]

.

The addition of filter ads

Filter aids can be mineral powders or organic fibrous materials, including diatomaceous, perlite and cellulose. It has been proved to have the abilities of increasing dust holding capacity, lowering particle releasing or shedding, but not increasing pressure

drop [49]. This explains why it has been applied to industry for over seventy years. Currently, there are two technologies adding filter aids, such as pre-coating and body-feeding. Pre-coating is to generate a thin filter aids layer, which helps to capture fine particles. Body-feeding is to blend the filter aids with the slurry and then they are fed to the filtration system together so that the formed filter cake can be more porous [50].

The addition of bacteria-destroying material

Koch et al. [47] added bacteria-destroying medication, such as an antibiotic or an iodophore to achieve the bacteria inhibition.

The extra nano-fiber layer

Fiber diameter is an essential parameter affecting filtration quality. Thinner fibers provide better filtration efficiency. Hence, nano-fibers have the potential to improve collection efficiency. Nano-fibers are defined as fibers with diameter range from 50 nm to 500 nm and can be made by electro-spinning process [51]. Comparing to conventional filter fibers, nano-fibers have higher surface area-to-weight ratio. Besides, the nano-fiber net-structure may act as active reaction sites, for example, the hygienic fictionalised filters, which are made from cationic polymers or incorporated with silver to kill bacteria [51]. It has been proved that the face mask prepared with nano-silver and an extra nano-fiber layer have the virus filtration efficiency (VFE) of 99.9% [51]. Recently, to decrease the pressure drop of nano-fibers, beaded and nano-fiber filters have been suggested. This is because the larger streamwire inter-fiber distance promotes air permeability and maintain high filtration efficiency [52]. Fig. 1.10 show the smooth (a) and beaded (b) nanofibers [52].

Hybrid filter fiber structures

Hybrid fiber webs with multi-components have been studied [53]. Zhang et al. [54] developed binary structure fibrous filters, which combine advantages of micro- and nabo-fibers and enhance filtration performance. Fig. 1.11a shows the fabrication process and components of the binary structure filter. Liu et al. [55] also produced

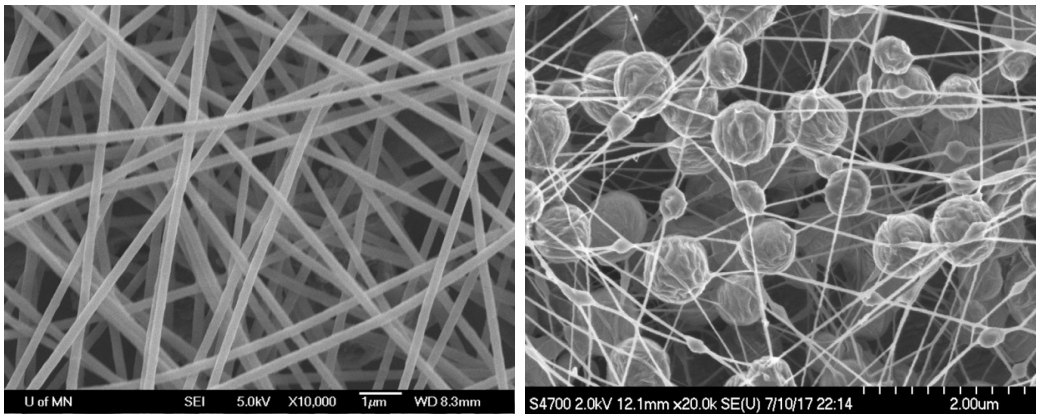

(a) (b)

Figure 1.10: Comparison of smooth nanofibers (a) and beaded nanofibers (b)[52]
.

air filtration products with ultra-high dust holding capacity and low resistance using bicompontent spunbond materials. Fig. 1.11 shows schematic processes of producing bicomponent filtration membranes using electrospinning and spunbond technology, respectively.

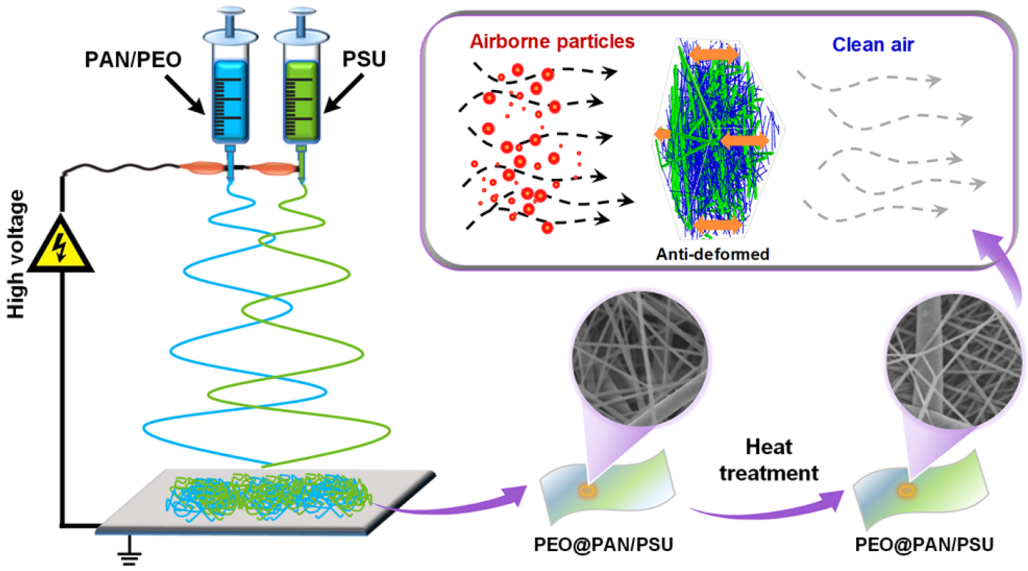

(a) Binary structure fibrous filters[54]

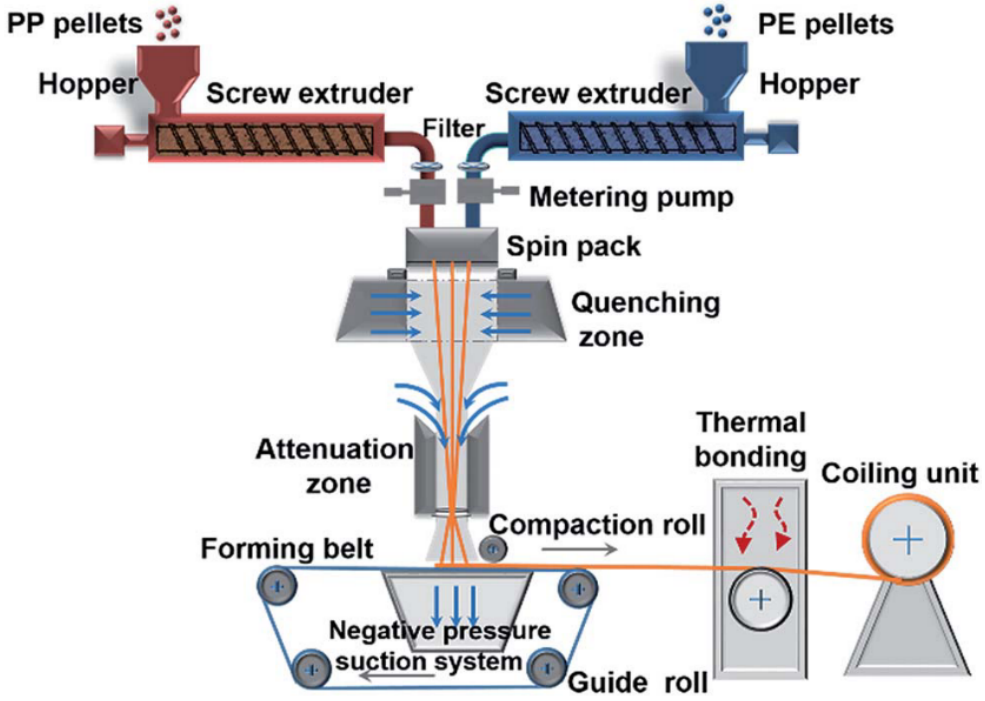

(b) Bicomponent spunbond process[55]

Figure 1.11: Multi-component filter structures

1.2.7 Bleached chemi-thermo mechanical pulping (BCTMP) wood pulp

As stated earlier, most commercial masks are made of polymers, such as polypropylene, polyurethane, polyacrylonitrile, polystyrene, polycarbonate, polyethylene, or polyester. These materials are difficult to be disposed and add vast plastic particle

waste in the environment [56]. In this case the low cost and environmentally friendly materials are more attractive.

Paper-based masks have been used to prevent the spread of infectious viruses before [57]. However, due to low efficiency and easiness of getting wet with saliva, such masks were not recommended as a precaution against droplets. On the other hand, wood pulp filters have some potential advantages, for example, they are inexpensive, environmentally friendly and easy to dispose of by incineration as a carbon-neutral fuel [58]. Besides, these days PAE (polyamide-amine-epichlorohydrin) has been used to provide wet strength to the filters [48]. PAE cross-links with the carboxyl group of cellulose and create stable covalent bonds, which provide the waterproof property [59].

Wood pulp fibers consist of fibrils, whose diameter ranges from a few microns to tens of nano-meters [58]. The nano-scale fibrillar structure has large specific surface, which makes it possible to capture small particles [60]. What is more, the fibrils can stable the filter structure. This property can be explained by the certain fibril angle, at which fiber-to-fiber bonds are formed [61]. These bonds prevent the accumulation of fibrous network, which may increase the pressure drop [58]. Many studies have forced on retaining pulp fibrillation by different drying processes, such as freeze-drying [62] and wet-beaten treatment [60]. Fibrillation happens in the refining processes. Fibrillar segments attached to fibers are also called fibrillation. It is of great importance because they are flexible and able to interact with other fibrils or neighboring fibers [53]. It has been proved that double disc refining results in the increase in fines formation, which is accompanied by the increase in fibrillation [53]. However, there has been no research using either chemi-thermo or mechanical or bleached chemi-thermo mechanical pulping (BCTMP) pulp to produce fibrous filters. Therefore, it may be possible to produce high efficiency air filters from BCTMP pulp.

1.3 Research objectives

Previous research mainly focused on developing novel treatment methods, for example mechanical treatment to expose the pulp fiber specific surface fibrils of wood pulp fibers, so that particle collection efficiency will improved. However, there is no research using pulp after being treated by multiple treatment to produce high efficiency air filters.

In this case, the objectives are firstly to produce pulp filters from pre-treated wood pulp and to characterize properties of different grades of pulp and pulp filters. For the pulp filter properties, pressure drop, which reflects breathing resistance, and particle collection efficiency. We also expect to study the morphology information of filters layers to see if particles are collected and how they are captured.

Chapter 2

Experiments

2.1 Experiment materials

Table 2.1: Experimental materials and information

Experimental materials	Information
Softwood pulp	Product # 625-75-00-10; Lot # 1C0372
Hardwood pulp	Product # 400-80-100-11; Lot # 2K9140
Whatman filter papers	CAT # (a) 1821-090 & (b) 1450-090
Commercial N95 masks	Produced by 3M; Lot # B18365 Product # TC-84A-0006
Candles	Watson's candles bought in Dollarama
Activated carbon powder	Cas # 7440-44-0
Incense sticks	
90.25% Ethanol	
Airbags	1 & 5L

Experimental materials and equipment include table 2.1, air, a vacuum pump and a digital manometer.

2.2 Experimental setups

The pulp filter producing setup consists of following units: a blender, a pulp suspension container, a funnel, and a conical flask connected to a vacuum pump, shown in Fig. 2.1a. The blender on the top is used to stir pulp slurry in the container. There is a valve on the bottom of the container, where the pulp suspension can be released

to the funnel below. The funnel is sealed to a conical flask so that water can be collected after separating from the mixture. There is also vacuum pump connected to the conical flask on the right (not shown in the picture) to shorter the drainage time.

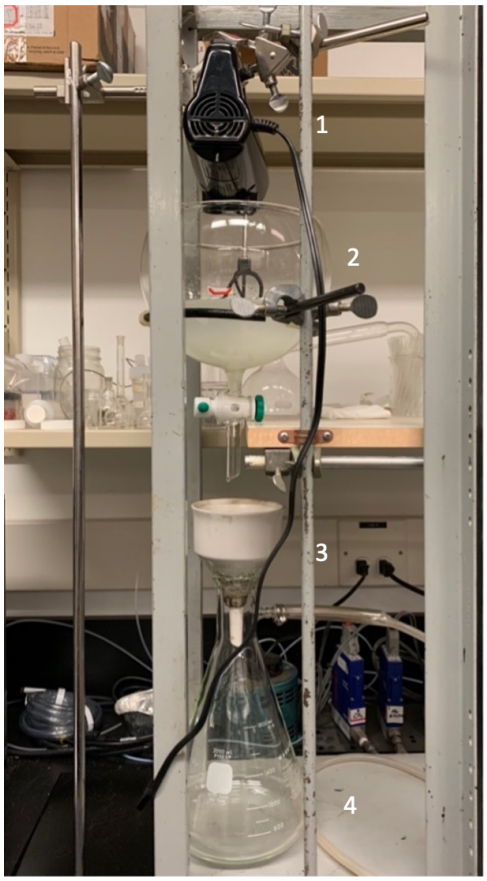

1. Blender

2. Container

3. Funnel

4. Conical flask

(a) Pulp filter production

1. Filter media 2. Manometer

(b) Pressure drop measurement

1. Filter media 2. Airflow carrying particles

(c) Particle deposition

Figure 2.1: Experimental setups for filter producing (a), pressure drop measurement (b), and filter capacity testing (c)

The experimental setups for pressure drop measurement and filter capacity comparison are similar. For the pressure drop measurement, there are two vertical and horizontal tubes. Filter media are put between the big horizontal tubes on the top. The pressure drop values were read from the manometer connected parallel to filter media. Airflow carrying particles goes through the vertical tubes, the upstream tube, filter media and downstream tube. (shown as the white arrow in Fig. 2.1b). For filtration efficiency tests, when particles are activated carbon powder, the powder is put at the bottom of the vertical tube in Fig. 2.1b. Airflow goes through the carbon powder, upstream of the horizontal tube and filter media to downstream tube. When using candle smoke, the bottom-side of the vertical tube is replaced by a burning candle. Air carrying candle smoke is exhausted by a vacuum pump connected to the other side of the burning candle so that candle smoke can be sucked and pass through filter media located between the horizontal tubes, as shown in Fig. 2.1c. The candle is put on an adjustable stage so that as it gets shorter during burning, the flame could stay on the same position.

2.3 Experimental methods

2.3.1 Pulp filter production

Initial fabrication of pulp filters

Wood pulp filter pads were produced by draining different volumes or mass concentrations of pulp slurry and dried in an oven at 95^oC for at least 24 hours after separated from Whatman filter papers. Then thickness of each sample was recorded. When releasing slurry from the container, the valve was widely open until the funnel was nearly 90% full. Then the valve was widely opened when the funnel was around 70% fulfilled with suspension. After that the valve was closed until the funnel was 90% full again so that the left suspension layer could be a protection of the filter pad surface from the impact of the flow. This process was repeated until the expected volume of suspension was drained.

The mass concentrations were 0.3 and 0.4% consistencies. And volumes were 0.5, 0.75 and 1 L, respectively. They were controlled by two methods: a) a specific

volume of suspension was made and drained; b) 2 L of suspension was made and put in the container, after that a specific volume of slurry was released from the container after stirring well, and the filter pad was removed. This process was repeated until all slurry was released. The filter papers used while draining were two grades of Whatman filter papers depending on filtration rates. For hardwood pulp, filter paper (b) was used because of smaller particle retention diameter, which provides pulp filter pads enough time to settle down evenly, while filter (a) was used to drain hardwood pulp. Whatman filter paper (a) & (b) have different filtration materials such as cellulose and glass microfibers, respectively. Particle retention diameters are 2.7 and 10 μm for filter paper (a) & (b). Lower drainage rate gives relatively smooth and homogeneous filter pads. This rate could also be controlled by opening or closing the vacuum pump.

Advanced development of pulp filters

The advanced pulp filters were provided by the cooperated company, Millar Western Forest Products Limited, to improve physical properties of pulp filters. Lab-made filter pads were fragile, especially being cut into small pieces. The advanced produced pulp filters are more flat, smooth and homogeneous. These filter samples include pressed and unpressed softwood and hardwood pulp filter sheets.

2.3.2 Initial pressure drop measurement and comparison

Flow rate and face velocity determination

The flow rate was controlled by adjusting the pressure settings and approximately measured by recording time consumed to fulfill a 1 or 5 L airbag. The pressure settings ranged from 30 to 50 psi with a $5-psi$ interval. Face velocity is determined by dividing flow rate by the effective exposed filter area, which is a circular place with a diameter of 5 cm in our experiments.

Pressure drop of pulp filters and commercial N95 masks

The pressure difference between the upstream and downstream of filter media was measured at different challenging face velocities (about 4, 10, 13, 17 cm/s). It

was conducted to single- and double-layer pulp filters as well as N95 masks for comparison. At each face velocity, four values were recorded. Each experiment was repeated 3 times. Graphs as a function of face velocity were plot with error bars representing standard deviations.

Pressure drop of new combined filter media

Considering different functions of N95 layers, it would be more comparable if the pulp filter sheet is a replacement of one layer of N95 masks. Therefore, a combination of N95 layers and pulp filters was used. Novel multi-layer filter media consist of two original layers of N95 masks and a single-layer of pulp filter. This filter sheet is made of pressed soft- or hardwood pulp. The construction of filter media is shown in table. 2.2. Other experimental situations were the same. Experiments were repeated three times. Pressure drop graphs were plot against face velocities with error bars representing standard deviations.

Table 2.2: Construction of all filter media (HW & SW represent hardwood & softwood pulp filter, $N95_1$, $N95_2$ & $N95_3$ mean the 1st, 2nd and 3rd layer of an original N95 mask)

Name	1st layer	2nd layer	3rd layer
Filter (a)	$N95_1$	$N95_2$	$N95_3$
Filter (b)	Pressed HW	$N95_1$	$N95_2$
Filter (c)	$N95_1$	Pressed HW	$N95_3$
Filter (d)	$N95_1$	$N95_2$	Pressed HW
Filter (e)	Pressed SW	$N95_2$	$N95_3$
Filter (f)	$N95_1$	Pressed SW	$N95_3$
Filter (g)	$N95_1$	$N95_2$	Pressed SW

2.3.3 Filtration efficiency comparison

To compare the capture efficiency of different filter media, the experiments were conducted by comparing the weight difference of filter layers pre- and post-exposed to particles. Challenging particles were activated carbon, powder candle smoke and incense stick smoke. The reason for choosing them is that the activated carbon

powder has the diameter around 500 nm, which is close to the infectious aerosols [63], and the candle smoke size is close to the MPPS (300 nm).

Particle selection, preparation and characterisation

A) Activated carbon powder

The activated carbon powder was mashed through a 20 μm sieve and collected at different flow rates (2, 5, 12, 15 L/min) by two methods: 1) Particles were collected consecutively without changing or adding new carbon powder while adjusting pressure settings; 2) Carbon powder was captured at various flow rates separately. Particles were removed after one collection and fresh particles were added. After collections, particles were dispersed into 90.25% ethanol with mass concentration of approximate 0.1% consistency. The particle size distribution (PSD) was analysed by Zetasize Nano based on light scattering.

B) Candle and incense stick smoke

Some researchers believe that candle smoke diameter at incomplete combustion mode is 270 ± 30 nm, while steady burning produces particles at approximate 25 nm in diameter [42]. The incense stick smoke has the diameter of 160 nm [40].

Particle filtration tests

When using activated carbon powder, about 0.2 g particles were put at the bottom of the vertical tube and blown to filter media at 5 & 12 L/min, for weight comparison and filtration process analysis, respectively. Duration time was 40 s. After that particles left in the vertical tube and the upstream tube were collected and weighed, separately. When using candle smoke, a burning candle was kept at incomplete combustion mode. Air and smoke were exhausted by a vacuum pump to the other side of the burning candle. Duration time varies (5, 30 and 50 min) to make sure that there was not too many particles captured by fibers, which results in the formation of filter cake and filtration process could not be seen clearly under either digital or scanning electron microscope. And there should be enough particles collected for weight comparison. During the experiment, candle was put on an adjustable metal

stage and moved up as burning so that the flame was at almost the same place and smoke could be fully exhausted to filter media. Also almost the same amount air was around the flame to keep candle at the same burning condition, the sooting mode [42], so that smoke can be generated.

Experiments were done on multi-layer of pulp filters and all filter media mentioned in table 2.2. Weight difference of each layer pre- and post-exposed to particles as well as the candle and activated carbon powder weight loss were recorded. Optical images and SEM images of filters with and without particle deposition were also captured.

Considering the size of ultra-fine particles, incense stick smoke was also tried. However, it was extremely hard to see the particles captured on all filter media under either digital microscope or SEM.

2.3.4 Morphology information of filter media

The morphology of filter media was studied by taking optical and SEM images before and after exposing them to particles. Images were taken by a digital microscope (Keyence VHX-2000) and the scanning electron microscope (Zeiss Sigma 300 VP-FESEM) at different magnifications and voltage settings. Lower voltage gives better morphology information, while higher voltage provides composition of materials. In SEM analysis, samples were coated with carbon or gold to make samples conductive. The composition was determined by the energy dispersive X-ray spectroscopy (EDS) analysis. To get clear morphology information, there should be enough but no too many particles on samples, so that particle cake has not formed and particles can be seen stuck on fiber surface. Therefore, for candle smoke deposition, the exposure time was set as 5 min, and for activated carbon powder tests, the flow rate was 2 L/min with the opening time of 40 s.

In addition, visual pictures were also captured. The darkness shows the evidence of collected particles. Though the evidence can be seen on visual pictures, it may not be seen under either digital or scanning electron microscope.

(a) Optical microscope

(b) Scanning electron microscope

Figure 2.2: Pictures of digital microscope (VHX-2000) and scanning electron microscope (Zeiss Sigma 300 VP-FESEM)

Chapter 3

Results & Discussions

3.1 Characterization of commercial N95 masks and pulp filters

Table 3.1 shows the information of commercial N95 masks, including thickness and basis weight. All three layers have almost the same thickness but different basis weights. The inner layer is the thickest and has largest basis weight. Basis weight can to some extent reflect filtration performance. Larger basis weight increases both filtration efficiency and pressure drop. It is attributed to the fact that larger mass (or thicker) pulp filter sheets have larger surface area of fibers [58].

Table 3.1: Information of N95 masks

	inner layer	middle layer	outer layer	Total
Thickness (mm)	1.0	0.7	0.9	2.6
Basis weight (g/m^2)	134.66	128.12	71.88	334.66

Fig. 3.1 shows initial and advanced produced pulp filter sheets. Pulp filter sheets provided by the cooperated company include pressed and unpressed hardwood and softwood pulp filters. They are smoother and more homogeneous. Information of advanced produced pulp filter sheets is shown in table 3.2

Fig. 3.2 shows the approximate relationship between thickness, volume and concentration of softwood and hardwood pulp suspensions. Since the pulp cannot be solved and the suspension is not exactly homogeneous, there is no linear relationship. Pulp tends to be stirred to the surface of the suspension, stick to the container wall, and cannot be released until all suspension is drained. Therefore, when a spe-

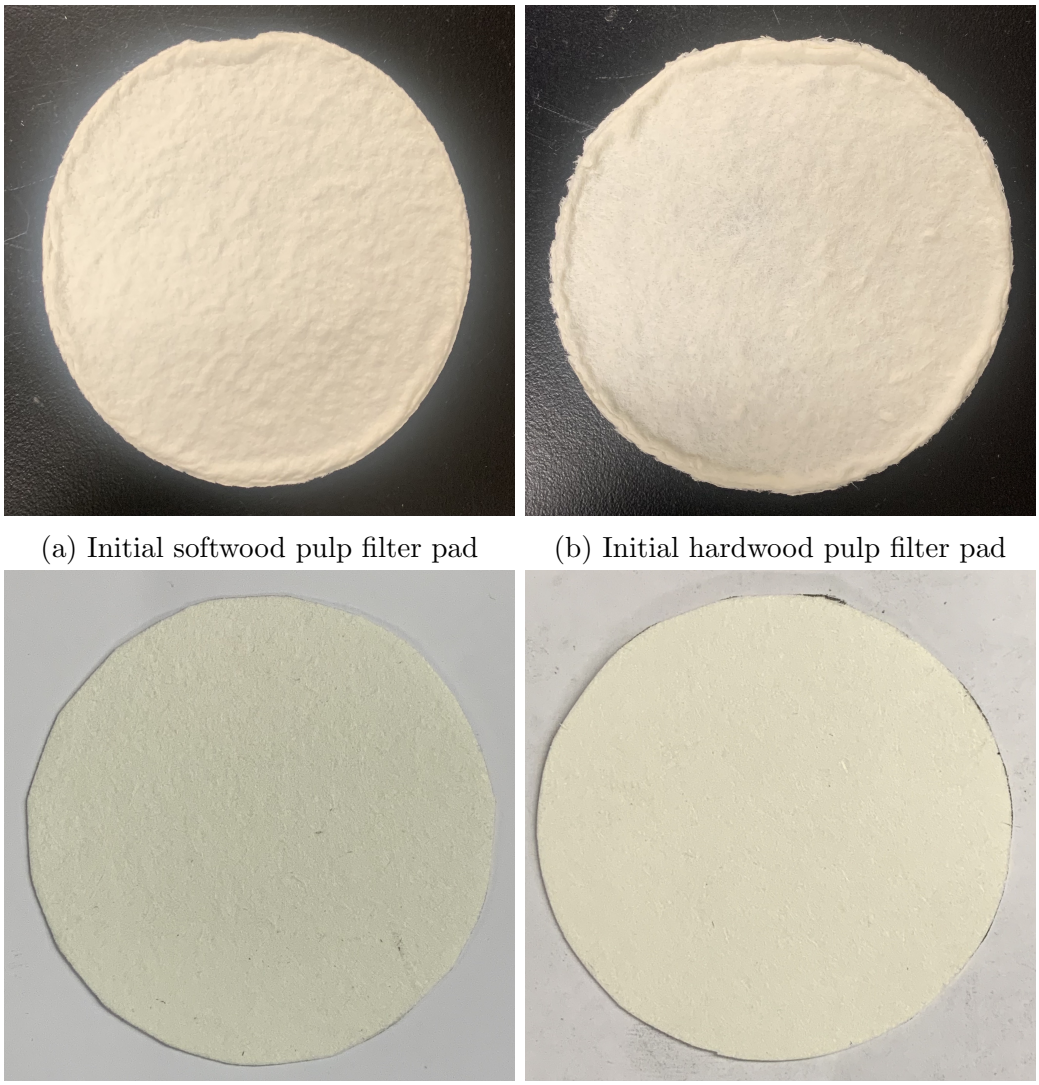

(a) Initial softwood pulp filter pad (b) Initial hardwood pulp filter pad

(c) Advanced softwood pulp filter (d) Advanced hardwood pulp filter

Figure 3.1: Pulp filter sheets produced in lab and provided by company: (a) & (b) are made in our lab; (c) & (d) are provided by the company

cific volume of mixture being released from the whole suspension at a time, the last sample is always thicker. Also at the beginning, the suspension at the bottom is more condensed, the first circle sometimes gives thicker pulp filters.

Thickness of lab-made pulp filter pads varied from 2 to 5 mm depending on concentration, volume and grade of wood pulp. Comparing to commercial masks, pulp filters were too thick. To produce thin but not fragile filter pads, 0.5 L of 0.3% consistency slurry was used the most. Thickness could go down to 1.2 and 2 mm for hardwood and softwood pulp filters, respectively. It is certain that at the same volume and consistency, hardwood pulp filters are thinner than softwood ones.

Table 3.2: Information of pulp filter sheets

	Unpressed softwood pulp filter sheet	Pressed softwood pulp filter sheet	Unpressed hardwood pulp filter sheet	Pressed hardwood pulp filter sheet
Thickness (mm)	0.8	0.5	0.7	0.3
Basis weight (g/m^2)	60	60	60	60

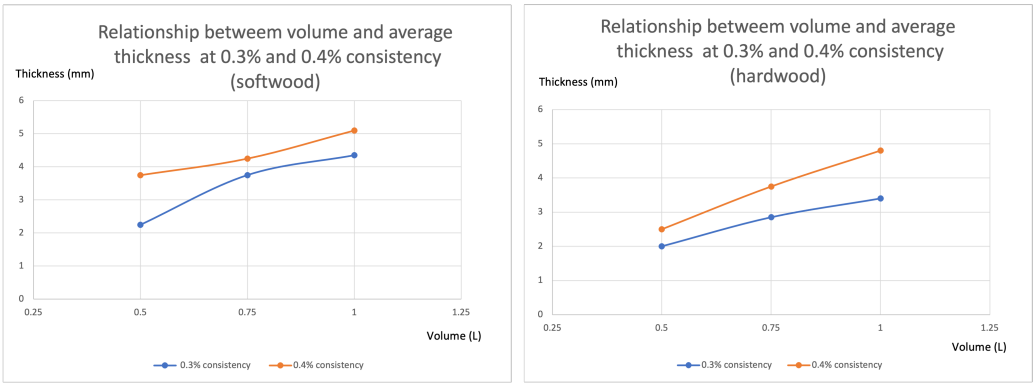

(a) Softwood pulp (b) Hardwood pulp

Figure 3.2: Relationship between thickness and suspension volume at different consistencies

This trend is constant to pulp filter sheets provided by the Millar Western Forest Products.

In comparison to company provided pulp filters, lab-made filters are thick, uneven and fragile. This is because of different production processes. Basis mechanism of producing filter papers from pulp is firstly draining the pulp and water mixture and drying the wet filter pads. The lab-made filter pads are dried in the oven for at least 24 hours. However, since pulp could not disperse in water evenly it was difficult to keep filter pads at a specific thickness. Besides, without pressing or modifying, the filter pads were rough textured and unevenly dense, for example there are small "hills" on filter pad surface. In comparison, the paper mill produces paper using advanced paper-making machine. It contain four sections. Firstly, pulp solution is injected at high pressure directly from the headbox into the space between two continuously rotating wires. Water is mainly removed by the following two sections, wet press section and dryer section. Water is squeezed out of the paper by pressure and then absorbed and carried away by wet felts. In the dryer section, heated

rollers are used to dry the paper. This process can also improve paper strength. Finally, paper passes through two finely polished steel cylinders, which precisely ensure the thickness is consistently even and then calenders make the paper surface extra smooth and glossy. For the N95 masks, they are mainly made of polypropylene fibers produced by spun bond and electro-spinning technologies [64].

3.2 Relationship between pressure setting, flow rate and face velocity

Table 3.3 shows the relationship between pressure settings and approximate flow rates. Flow rate is measured by recording the time to fulfill an airbag with a specific volume at a pressure setting. Thus, the relationship can be figured out. The effective exposed area in experiments was a circular area with a diameter of 5 cm. Based on the definition, face velocities can be calculated by dividing the flow rate by exposed area.

Table 3.3: Relationship between pressure setting, flow rate and face velocity

Pressure setting (psi)	Flow rate (L/min)	Face velocity (cm/s)
30	2	1.70
35	5	4.25
40	12	10.19
45	15	12.74
50	20	16.99

However, the flow rate measurement method is not accurate, because it is hard to tell whether the airbag is full or not. In other studies, airflow always comes from air cylinder with a fixed pressure setting and the flow rate is controlled by a ball valve and read from a flow meter, and there is also a bypass connected parallel to the filter section [58, 62].

3.3 Particle size distribution analysis

Table 3.4: Particle size distribution of carbon powder collected at different flow rates by two methods

Flow rate (L/min)	2	5	12	15
Peak mean diameter $d_1(nm)$ (roughly)	440	480	500	520
Peak mean diameter $d_2(nm)$ (roughly)	440	590	530	480

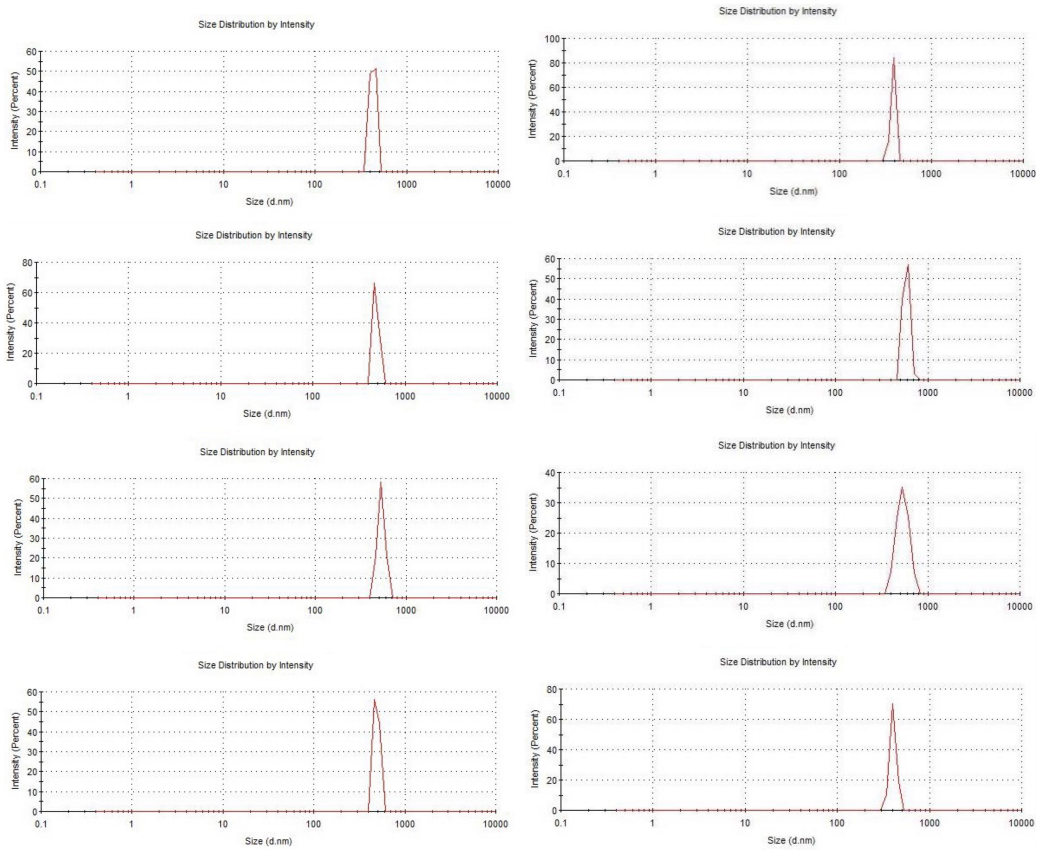

(a) Method 1 (b) Method 2

Figure 3.3: Size distribution of activated carbon powder collected at different flow rates by different methods: (a) samples collected consecutively (method 1), (b) samples collected separately (method 2); from top to bottom, collection flow rate increases

Size distribution of carbon powder collected at various flow rates is shown in Fig. 3.3 and peak diameters are shown in table 3.4. In fig. 3.3, from top to bottom flow rate increases. d_1 represents peak diameter of particles captured by method 1, which is adjusting flow rates without replacing particles with fresh ones. d_2 is the peak

diameter of particles collected by using new particles at each flow rate (method 2). There was only one peak in each size distribution graph, shown in fig. 3.3. Particles collected at 2 L/min by method 1 & 2 have the same peak mean diameter. When using method 1, at higher flow rates larger particles were collected, though the difference was not obvious. However, in method 2, where smaller particles have the opportunity to be collected by higher flow rates, the trend in diameter was opposite. 5 L/min gave the largest peak mean diameter, 590 nm. As flow rate increased, peak mean diameter decreased.

Theoretically, peak mean diameter increases as flow rate goes up. This trend is seen in particles collected by method 1. However, there is an opposite trend when using method 2. This might be because carbon powder could not dissolve in ethanol, particles coagulated, settled, and formed bigger particles. Thus, the light scattering results might be affected. This phenomenon is more likely to happen to smaller particles because of higher specific area according to the DLVO theory, which described particle-particle interaction mechanisms in detail [65].

3.4 Pressure drop comparisons

Graphs were plot as a function of face velocity with error bars. As face velocity increases, pressure drop goes up linearly. Softwood pulp filters have a relatively low pressure drop comparing to hardwood. Pressed filters experience higher pressure drop than fluffy ones. Pressed hardwood pulp filters exhibit the highest pressure drop, in contrast unpressed softwood pulp filters have the lowest pressure drop, shown in Fig. 3.4. Pressed softwood and unpressed hardwood pulp filter have similar pressure drop. The same experiments were also conducted on a double-layer pulp filters. Pressure drops were twice more than those of single-layer filters. The extra one layer of the same kind of filter doubles the pressure drop.

When one layer in an N95 mask was replaced by a pulp filter sheet, the new multi-layer filter media have higher pressure drops comparing to the N95 mask itself. It can be concluded that single-layer pulp filters are more air-resistant than every layer in N95 masks. And the middle layer in N95 masks contributes the most pressure

drop. There are few differences between other two N95 layers.

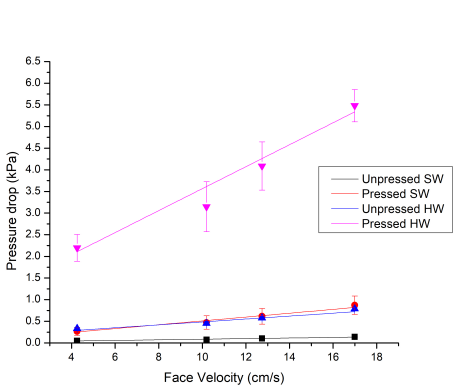

(a) Single-layer pulp filters

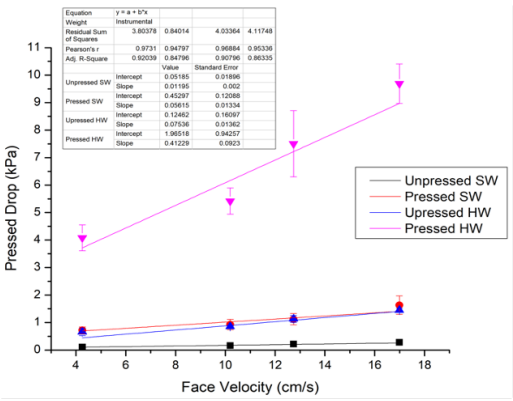

(b) Double-layer pulp filters

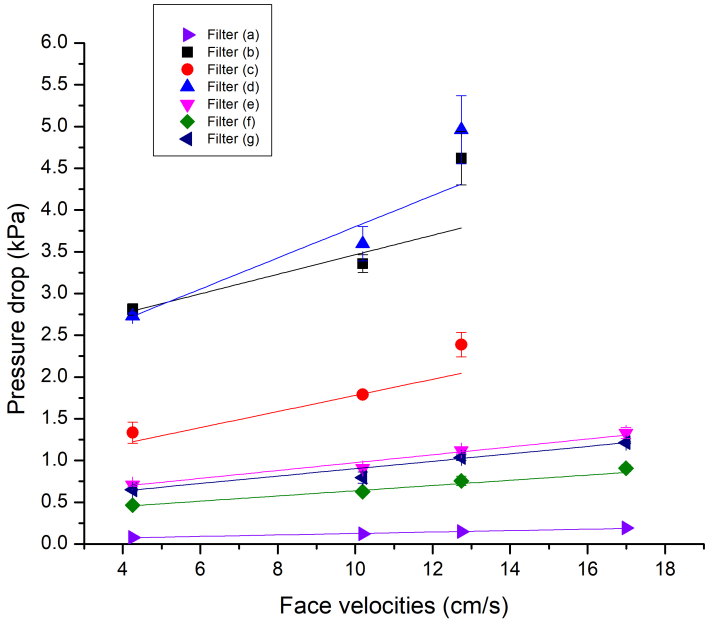

(c) Combined filter media and N95 mask

Figure 3.4: Pressure drop of pulp filters and all seven new filter media as a function of face velocity. (a) single-layer of pulp filter sheets; (b) double-layer of pulp filters; (c) new combined filter media and N95 masks

The results of pressure drop measurements agree with previous theories, wood pulp filters have higher pressure drops, because the loose fibrils are likely to accumulate [58]. And graphs also shows a linear relationship between pressure drop and face velocity, although there are little errors.

However,according to NIOSH standards [9], the initial inhalation and exhalation resistance should not exceed 245 and 343 Pa, respectively when the flow rate is 85

L/min, corresponding to the face velocity of about 8 cm/s. Neither pulp filters or combined filter media are qualified.

3.5 Filtration efficiency tests on pulp filters

3.5.1 Weight change after particle deposition

Activated carbon powder as challenging particles

Table 3.5 shows weight change of pulp filter media and carbon powder weight loss after filtration tests at two face velocities, 4.25 & 10.19 cm/s. At low flow rates, softwood pulp filters collected more particles than those made of hardwood pulp and fluffy filters blocked more carbon powder than pressed ones. While at a relatively higher gas velocity, hardwood pulp filters collected more particles.

Table 3.5: Weight change of pulp filters before and after activated carbon passing through and carbon powder weight loss

Face velocity (cm/s)	4.25		10.19	
	Filter weight gain (g)	Carbon loss (g)	Filter weight gain (g)	Carbon loss (g)
Unpressed softwood	0.0381	-0.1558	0.0353	-0.0755
Pressed softwood	0.0261	-0.1217	0.0411	-0.1039
Unpressed hardwood	0.0235	-0.0788	0.0451	-0.0892
Pressed hardwood	0.0103	-0.0994	0.0414	-0.1207

This result is opposite to previous studies, which have proven that filters with higher packing density or lower porosity have higher collection efficiency [43, 44]. The reason for this discrepancy can be explained by experimental errors. For examples, particles were not stably captured by filters. They were easy to fall off with a little collision. And not all carbon powder could be weighted after each run. There were some particles left in tubes.

Candle smoke as challenging particles

Table 3.6: Weight difference of pulp filters after exposure to candle smoke for $50min$

	1st layer (g)	2nd layer (g)	3rd layer (g)	4th layer (g)	Total (g)
Unpressed softwood	0.0072	0.0017	-0.0004	–	0.0085
Pressed softwood	0.0662	0.0128	0.0093	0.0056	0.0939
Unpressed hardwood	0.0336	0.0043	0.0038	0.0071	0.0488
Pressed hardwood	0.2136	0.0250	0.0193	0.0183	0.2768

When particles were candle smoke (see table 3.6), pressed pulp filters collected more particles, and hardwood performed better than softwood. Hence, pressed hardwood pulp filters filtered the most smoke, followed by pressed softwood pulp filters. The least particles were collected by the unpressed softwood pulp filter. First layers were the dominated layer in capturing candle smoke. The deeper the fewer particles collected, except the unpressed hardwood pulp filter. The last layer gained more weight than the 2nd and 3rd layer.

This result is consist to the theory that higher packing density higher collection efficiency. Hardwood has higher packing density than softwood. Pressed filters are also more condense than fluffy filters. The reason for the consistent results may be because candle smoke is more likely to be carried by airflow and the amount left in the upstream tube would be similar in each filtration experiment and it have no impact on candle weight loss. One of the experimental error avoided in these filtration tests.

3.6 Filtration efficiency tests on novel multi-layer filter

3.6.1 Activated carbon powder as challenging particles

Weight change after exposure to particles

Table 3.7: Weight change of filter media after deposited with activated carbon powder and carbon powder consumed

	1st layer (g)	2nd layer (g)	3rd layer (g)	Total (g)	Activated carbon (g)
Filter (a)	0.0245	0.0014	0.0004	0.0263	-0.1121
Filter (b)	0.0152	0.0005	0.0004	0.0161	-0.0909
Filter (c)	0.0282	-0.0039	0.0003	0.0246	-0.1100
Filter (d)	0.0201	0.0019	-0.0072	0.0148	-0.0758
Filter (e)	0.0355	0.0008	0.0002	0.0365	-0.1269
Filter (f)	0.0351	-0.0063	0.0007	0.0295	-0.0974
Filter (g)	0.0341	0.0017	-0.0084	0.0274	-0.1026

Table 3.7 shows weight change of each layer in novel filter media and carbon powder weight loss after filtration tests. In each filter media, the 1st layer facing particles dominated the whole filtration processes. Few carbon powder could penetrate into deep layers. The most particles were collected by filter (e), where the pressed softwood pulp filter sheet was used as the 1st layer. In contrast, filter (d) collected the least particles. When comparing filter (e), (f) & (g) and filter (b), (c) & (d), filter media containing softwood pulp layer captured more particles.

Photos of filter media pre- and post-exposure to particles

From photos, all filter media performed well on carbon powder filtration. Particles barely penetrated deep into the 3rd layers. First layers dominated the filtration processes in all filters. When comparing filter (a), (b) & (e), pulp filters played the most important role in collecting carbon powder. Few particles reached to the 2nd or 3rd layer. However, the middle layer in the N95 mask has been dark. When pulp filters were used as the a replacement of the original 2nd layer, all filter media

performed similarly, particles could barely seen on the last layer. This trend is also seen in filter (d) & (g), all filter media performed well. Thus, all filter media showed high filtration efficiency on activated carbon powder filtration. Pulp filters worked a little better than N95 layers. It is difficult to tell whether hard- or softwood pulp filters performed better. Combining the information in weight change of each layer after exposure to particles, softwood pulp performed better.

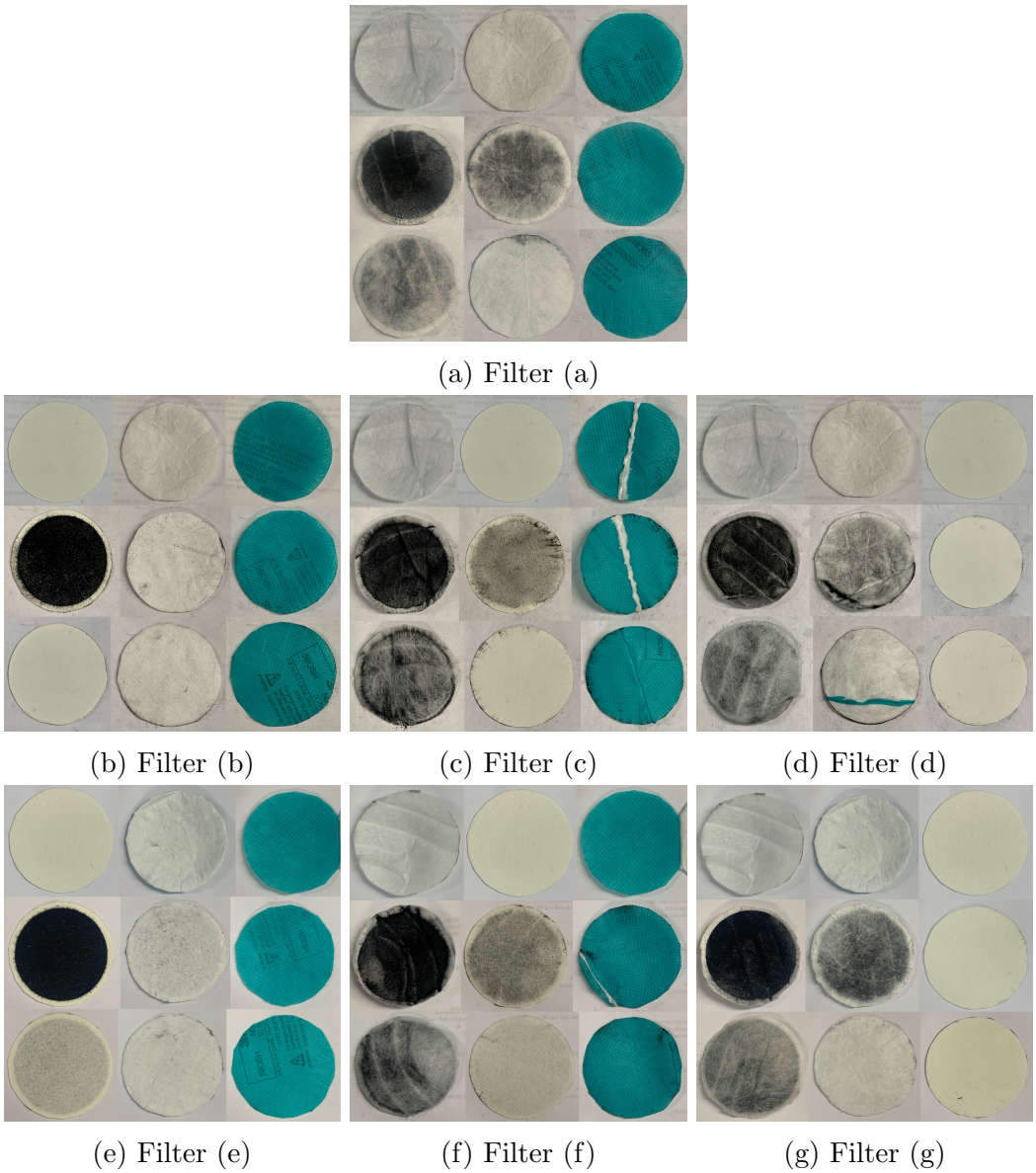

(a) Filter (a)

(b) Filter (b) (c) Filter (c) (d) Filter (d)

(e) Filter (e) (f) Filter (f) (g) Filter (g)

Figure 3.5: Photos of novel multi-layer filter media with and without carbon powder deposition

This result agrees with the filtration efficiency of pulp filters at relatively lower flow rate, but is opposite to the theory that filtration efficiency is proportional to

packing density. The reason for similar filtration efficiency may be because the concentration challenging particles was too low and did not reach filter media capacity, although it has exceeded NIOSH standard (200 mg/m^3) [8].

3.6.2 Candle smoke as challenging particles

Weight difference before and after particle deposition

Table 3.8: Weight difference of filter media pre- and post-exposed to candle smoke and candle weight decrease

	1st layer (g)	2nd layer (g)	3rd layer (g)	Total (g)	Candle (g)
Filter (a)	0.0161	0.1006	0.0044	0.1211	-5.4092
Filter (b)	0.2801	0.0160	0.0144	0.3105	-5.5249
Filter (c)	0.0428	0.0178	0.0052	0.0658	-4.7500
Filter (d)	0.0336	0.0081	0.0016	0.0433	-3.8640
Filter (e)	0.0144	0.0087	0.0023	0.0254	-3.9318
Filter (f)	0.0101	0.0350	0.0046	0.0497	-4.9020
Filter (g)	0.0079	0.0353	0.0020	0.0452	-5.0614

Table 3.8 shows weight gain of filter media and candle weight loss after burning for 50 min. Filter (b) collected the most particles, 0.3105 g. It is about three times more than that collected by the original N95 mask. When the 1st was the pressed softwood filter sheet, the least particles were collected. Filter media containing a layer made from hardwood pulp captured more particles than those with a softwood pulp filter layer. Thus, hardwood pulp filers performed better on candle smoke filtration than softwood. Wood pulp filters have higher collection efficiency than every layer in N95 masks. When comparing the weight gain of each layer in filter media, the middle layer in the N95 mask collected the most dust. For filter media including hardwood pulp filter layer, the 1st layer collected the most particles. When softwood pulp filter was used, the most particles were collected by the 2nd layer except for filter (e). Majority of candle smoke was collected by the 1st layer, the softwood pulp filter layer.

Photos of filter media with and without particles

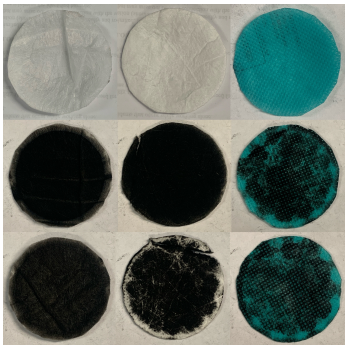

(a) Filter (a)

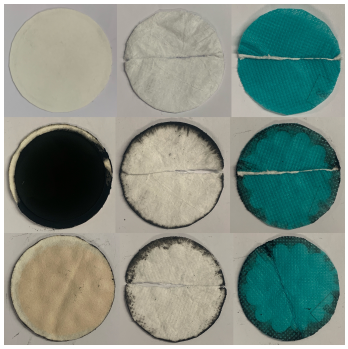

(b) Filter (b)

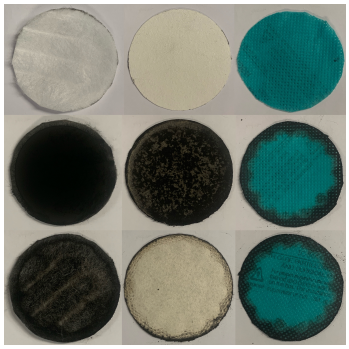

(c) Filter (c)

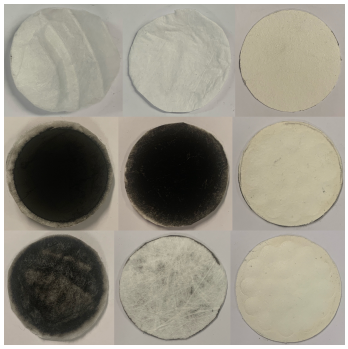

(d) Filter (d)

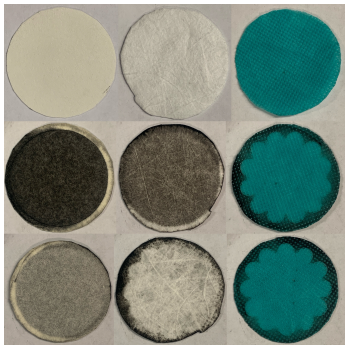

(e) Filter (e)

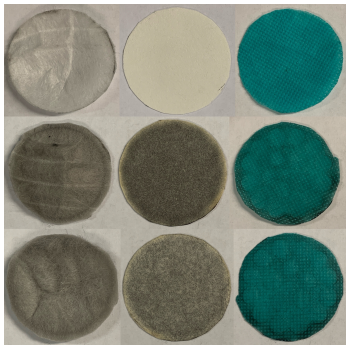

(f) Filter (f)

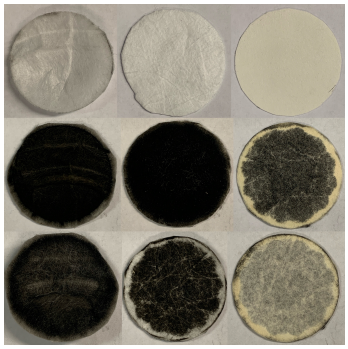

(g) Filter (g)

Figure 3.6: Photos of filter media before and after candle smoke deposition

Fig.3.6 shows photos of all filter media in table 2.2 before and after exposure to candle smoke. First rows from left to right are the 1st, 2nd and 3rd layers of clean filter media. The second and third rows are the front and back of filters with candle smoke deposition. In the commercial N95 mask, particles have penetrated to the last layer. When hardwood pulp filter was used, few particles could pass through or reach that layer. When softwood pulp filter was used, particles could barely went through. While when it was used as the last layer, filter (g), more particles penetrated into it.

Photos gave the same conclusion as the weight change table, pulp filters showed better performance than N95 layers and hardwood worked better than softwood.The result is also consistent to collection efficiency tests on pulp filters and proves that filters having higher packing density show higher collection efficiency.

To summary, when challenging particles were activated carbon powder, all filter media performed higher filtration efficiency. This may be because the total amount of dust was also lesser than candle smoke, and carbon powder has larger diameter (about 500 nm) than candle smoke (about 300 nm), which is around the most penetrating particle size (MPPS). Wood pulp based filters showed better performance than N95 layers on ultra-fine particle filtration. This result agrees with the previous research on pulp based filters for removal of sub-micrometer aerosol particles. It has proved that pulp filters are capable to remove fine particles from air and for pressure drop, they are also comparable to N95 masks [58].

3.7 Morphology and composition

3.7.1 Optical images

Pulp filters

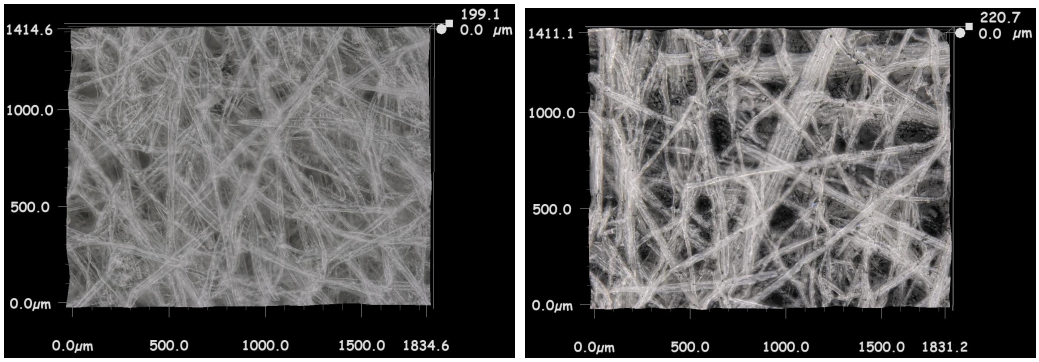

(a) Before candle smoke deposition (b) After candle smoke deposition

Figure 3.7: Optical images of pressed softwood pulp filter with and without particle deposition

Fig. 3.7 shows the pressed softwood pulp filter before and after exposure to candle smoke for $5min$. The magnifications are 500x. Comparing to the blank pulp filter image, the black spots stuck in pores and between fibers in fig. 3.7b are believed to

be captured particles. Since the exposure time was short, only few particles were blocked and seen on fibers, and particle cake did not form, otherwise only a carbon cake could be seen. For other challenging particles and pulp filters, images were similar. However, filters that are too condense, for example the pressed hardwood pulp filter, cannot be seen clearly using optical microscope.

N95 filters

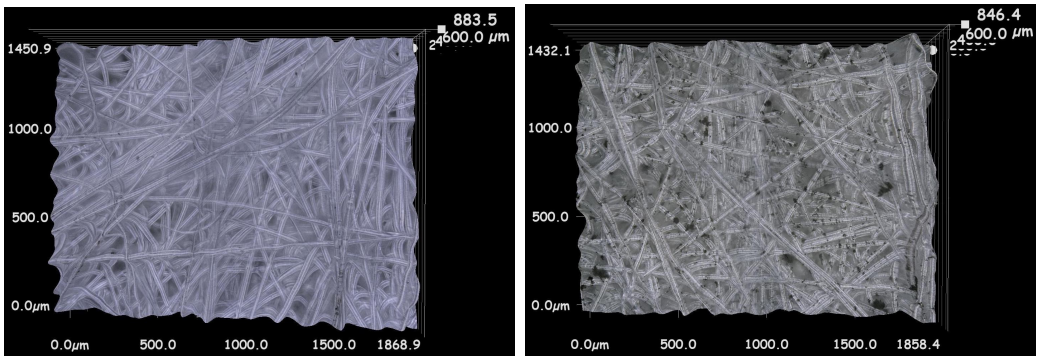

(a) 1st layer of a clean N95 mask (b) 1st layer of an N95 mask with smoke

Figure 3.8: 1st layer of an N95 mask pre- and post-exposed to candle smoke for $5min$

Fig. 3.8 shows the inner layer of N95 masks before and after exposure to candle smoke for only 5 minutes. Comparing to fig. 3.8a, black spots in fig. 3.8b are believed to be collected particles. Similarly as pulp filters, particles were stuck on fiber surface. Images of the 3rd layer look the same. While the middle layer could not be seen clear under optical images. This is because it has thinner fibers and is more condense. And the cap-shape of N95 masks make is more difficult to be focused on. Thus, we moved on to scanning electron microscope.

3.7.2 SEM images

N95 filters

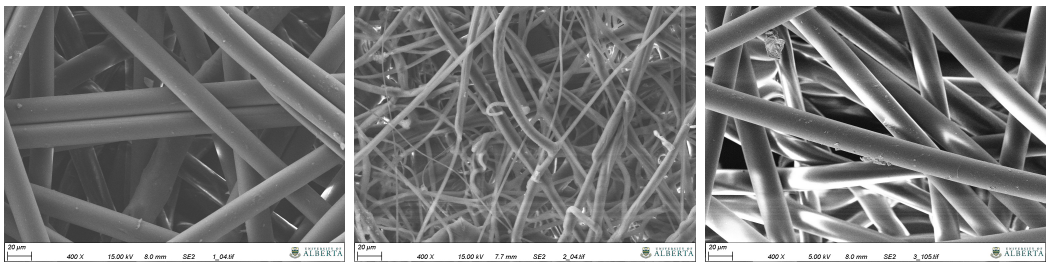

(a) Inner layer (b) Middle layer (c) Outer layer

Figure 3.9: SEM images of a clean N95 mask

Fig. 3.9 shows SEM images of each layer in an N95 mask. The 1st & 3rd layer have similar structure and fiber diameter. Fiber diameters in the middle layer are smaller. And this layer also looks condense than the other two layers. This is the evidence showing that the 2rd layer is the filter layer, while other two layers are support layer and also explains why it has relatively higher pressure drop.

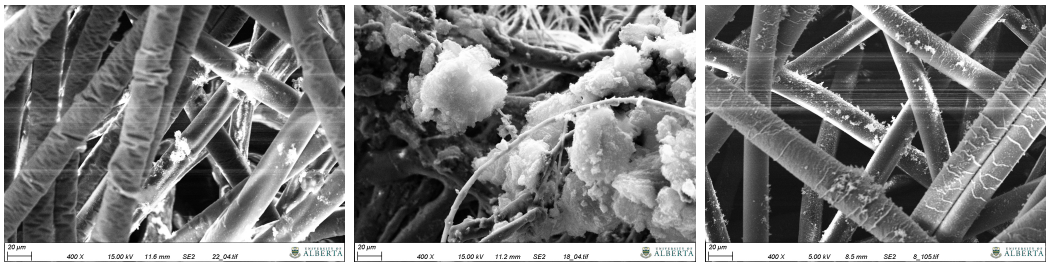

(a) Inner layer (b) Middle layer (c) Outer layer

Figure 3.10: SEM images of N95 filters with particle deposition

Fig. 3.10 shows each layer in an N95 mask with particle deposition. Particles aggregate together and are captured on fiber surface. The bright spots are believed to be particles.

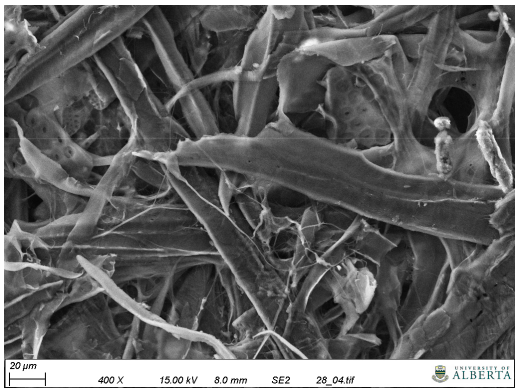

(a) Softwood pulp filter (clean)

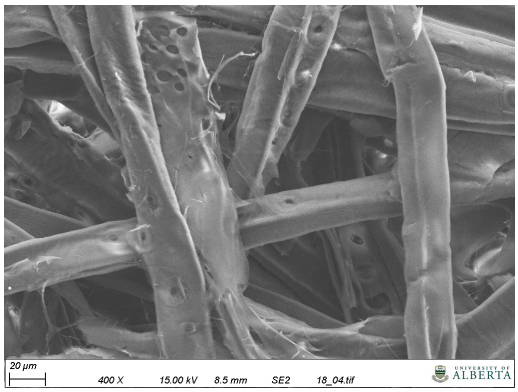

(b) Hardwood pulp filter (clean)

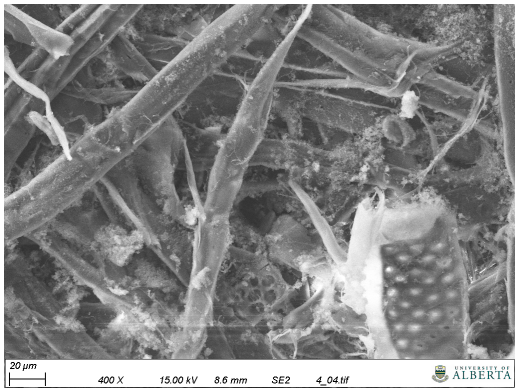

(c) Softwood pulp filter (with particles)

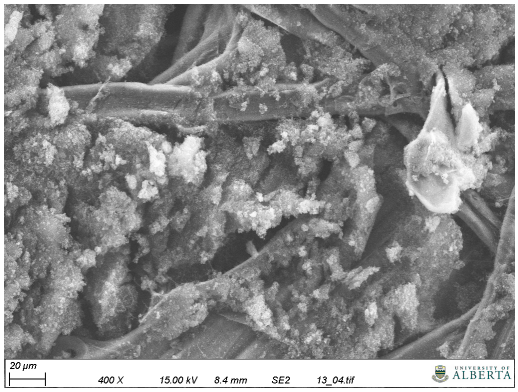

(d) Hardwood pulp filter (with particles)

Figure 3.11: SEM images of pulp filters with and with particles

Pulp filters

3.7.3 Images of challenging particles

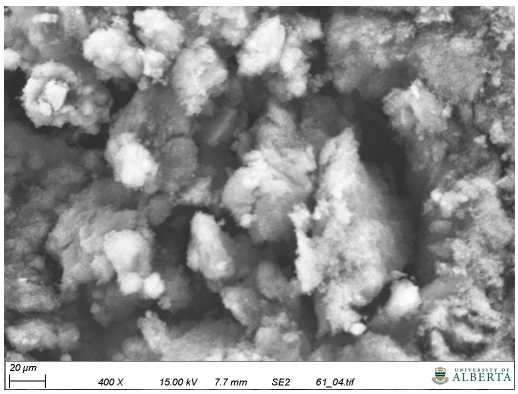

(a) Candle smoke

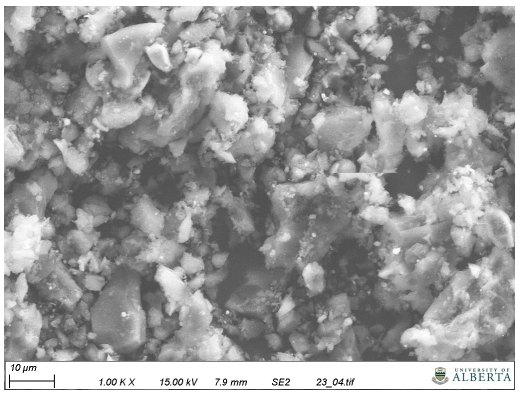

(b) Activated carbon

Figure 3.12: SEM images of particles used in experiments

Fig. 3.12 shows images of candle smoke and activated carbon under SEM. Both of them look fluffy. Candle smoke is more likely to coagulate together comparing to activated carbon.

By comparing SEM images of filter layers with and without particles as well as challenging particles. Bright spots on fiber are believed to be collected particles. This also can be proved by the EDX-analysis. It gives the composition of specific areas. For example the inner layer consists of 65% carbon and 35% oxygen, the bright spots and challenging particles contains at least 90% carbon. For pulp filters, the carbon composition increased from 59% to 70% after exposure to particles. However, this method does not work on the middle or 3rd layer of N95 masks. These layers are made of polypropylene, which only composed of carbon and hydrogen.

The images also gives approximate information of packing density. Pulp filters look more condense they every layer in N95 masks, and hardwood pulp filters also have lower porosity than those made from softwood pulp. This explains why pulp filters, especially hardwood pulp filters have quite high pressure drop.

Chapter 4

Conclusions and future work

4.1 Conclusions

In this thesis, we characterized properties of different grades of wood pulp and pulp based filters. For the pulp filters we focused on their pressure drop and particle collection efficiency, and then made a comparison with commercial masks. After that we studied the morphology information of pulp filters, N95 filters and challenging particles used in this research, activated carbon powder and candle smoke.

Pulp filters show higher pressure drop than N95 layers. The one piece of pressed hardwood pulp filter sheet has the pressure drop of about 3 kPa, and the smallest value, approximate 200 Pa, belongs to the unpressed softwood pulp filter, when the face velocity is about 10 cm/s. After comparing the ability of particle removal from air using activated carbon powder and candle smoke, pressed filters show better filtration efficiency. Thus, they have been chosen as the alternative layers, though they have relatively higher pressure drop.

Novel multi-layer filters have been produced. They are composed of one piece of pressed hard- or softwood pulp filter sheet and two original N95 layers. The same pressure drop and collection efficiency tests were conducted on these novel filter media. Filter media containing pressed hardwood pulp filter sheet and the N95 middle layer show higher pressure drops, about 3.5 kPa at 10 cm/s. The lowest pressure drop value, about 500 kPa, belongs to filter (f), which contains the N95 inner and outer layer and the pressed softwood pulp filter sheet as the 2nd layer. However, it is still larger than the NIOSH standard for commercial high efficiency

air filters.

In the filtration efficiency test, pulp filters performed better than every layer of N95 masks on both activated carbon powder and candle smoke. When pulp filters were used, the last layer after exposure to particles were always clean. While for the original N95 mask, there were plenty of particles on them, especially after candle smoke filtration tests. And the most particles were collected by filters with pulp filters as their 1st layer. Hardwood pulp filters performed better on candle smoke filtration tests, while softwood showed higher capture efficiency when using carbon powder. The later result needs more investigation since it is opposite to the theoretical predictions.

For the morphology information studies, particles were collected by fiber surface and seen under optical and scanning electron microscope. Particle dendrites have formed.

Hence, pulp filters have the ability of removing particles from air and collecting them by pulp fibers. Though they show higher pressure drop, they are a strongly competitive material to the current used synthetic polymer. This is also because pulp filters are biodegradable and inexpensive. Also comparing the spun-bond and electro-spinning technologies, pulp filter production processes are much easier and mature.

4.2 Future work

In the future work, it is essential to reduce the pulp filters pressure drop. Comparing to NIOSH standard and considering the comfort of wearing, the pressure difference between the upstream and downstream should be lower than 343 Pa [9]. This could be achieve by adjusting weight density and/or thickness. We also need to improve the experimental setups to accurately measured filtration performance. For example, in candle smoke filtration test, it is necessary to keep candles at the same burning condition so that the smoke concentration would be the same. Beside, during the candle combustion, there are water and heat generated. The impact on filtration performance caused by environmental situation change should be reduced. We also

expect to investigate incorporation of nano-carbon/nano-silver or some oxidizing materials to kill bacteria or viruses.

Bibliography

[1] C. J. Kahler and R. Hain, "Fundamental protective mechanisms of face masks against droplet infections," *Journal of Aerosol Science*, vol. 148, p. 105 617, 2020, ISSN: 0021-8502. DOI: https://doi.org/10.1016/j.jaerosci.2020.105617. [Online]. Available: https://www.sciencedirect.com/science/article/pii/S0021850220301063.

[2] G. Leung, T.-H. Lam, L.-M. Ho, S.-Y. Ho, B. H. Y. Chan, I. O. L. Wong, and A. Hedley, "The impact of community psychological responses on outbreak control for severe acute respiratory syndrome in hong kong," *Journal of epidemiology and community health*, vol. 57, no. 11, pp. 857–863, 2003, ISSN: 0143-005X. DOI: 10.1136/jech.57.11.857. [Online]. Available: https://europepmc.org/articles/PMC1732323.

[3] I. M. Hutten, "Chapter 5 - processes for nonwoven filter media," in *Handbook of Nonwoven Filter Media (Second Edition)*, I. M. Hutten, Ed., Second Edition, Oxford: Butterworth-Heinemann, 2016, pp. 276–342, ISBN: 978-0-08-098301-1. DOI: https://doi.org/10.1016/B978-0-08-098301-1.00005-8. [Online]. Available: https://www.sciencedirect.com/science/article/pii/B9780080983011000058.

[4] S. Dharmaraj, V. Ashokkumar, S. Hariharan, A. Manibharathi, P. L. Show, C. T. Chong, and C. Ngamcharussrivichai, "The covid-19 pandemic face mask waste: A blooming threat to the marine environment," *Chemosphere*, vol. 272, p. 129 601, 2021, ISSN: 0045-6535. DOI: https://doi.org/10.1016/j.chemosphere.2021.129601. [Online]. Available: https://www.sciencedirect.com/science/article/pii/S0045653521000710.

[5] T. A. Aragaw, "Surgical face masks as a potential source for microplastic pollution in the covid-19 scenario," *Marine Pollution Bulletin*, vol. 159, pp. 111517 –111 517, 2020.

[6] H. Chowdhury, T. Chowdhury, and S. M. Sait, "Estimating marine plastic pollution from covid-19 face masks in coastal regions," *Marine Pollution Bulletin*, vol. 168, p. 112 419, 2021, ISSN: 0025-326X. DOI: https://doi.org/10.1016/j.marpolbul.2021.112419. [Online]. Available: https://www.sciencedirect.com/science/article/pii/S0025326X21004537.

[7] S. Saadat, D. Rawtani, and C. M. Hussain, "Environmental perspective of covid-19," *Science of The Total Environment*, vol. 728, p. 138 870, 2020, ISSN: 0048-9697. DOI: https://doi.org/10.1016/j.scitotenv.2020.138870. [Online]. Available: https://www.sciencedirect.com/science/article/pii/S0048969720323871.

[8] A. N. Aft, "42 CFR PART 84 STANDARD," *TSI Incorporated*, pp. 84–86, 1995.

[9] Cho, "Pressure Drop Of Filtering Facepiece Respirators: How Low Should We Go?" *Physiol. Behav.*, vol. 176, no. 1, pp. 100–106, 2016. DOI: 10.13075/ijomeh.1896.00153.PRESSURE.

[10] S. Ishack and S. R. Lipner, "Applications of 3d printing technology to address covid-19–related supply shortages," *The American journal of medicine*, vol. 133, no. 7, pp. 771–773, 2020.

[11] J. Dhivyadharshini, J. Somasundaram, and M. Brundha, "Composition and uses of n95 masks -a review," English, *European Journal of Molecular and Clinical Medicine*, vol. 7, no. 1, Dec. 2020.

[12] National Personal Protective Technology Laboratory, "Determination Of Particulate Filter Efficiency Level For N95 Series Filters Against Solid Particulates For Non-Powered, Air- Purifying Respirators Standard Testing Procedure (Stp)," *Natl. Inst. Occup. Saf. Heal.*, pp. 1–11, 2012.

[13] J. Mao, B. Grgic, W. H. Finlay, J. F. Kadla, and R. J. Kerekes, "Wood pulp based filters for removal of sub-micrometer aerosol particles," *Nordic Pulp & Paper Research Journal*, vol. 23, no. 4, pp. 420–425, 2008. DOI: doi: 10.3183/npprj-2008-23-04-p420-425. [Online]. Available: https://doi.org/10.3183/npprj-2008-23-04-p420-425.

[14] P. T. O. Shaughnessy, B. Strzelecki, M. Ortiz-Hernandez, P. Aubin, X. Jing, Q. Chang, J. Xiang, P. S. Thorne, and J. T. Stapleton, "Characterization of performance and disinfection resilience of nonwoven filter materials for use in 3d-printed n95 respirators," *Journal of Occupational and Environmental Hygiene*, vol. 18, no. 6, pp. 265–275, 2021, PMID: 33989113. DOI: 10.1080/15459624.2021.1913283. eprint: https://doi.org/10.1080/15459624.2021.1913283. [Online]. Available: https://doi.org/10.1080/15459624.2021.1913283.

[15] C Huang, K Willeke, Y Qian, S Grinshpun, and V Ulevicius, "Method for measuring the spatial variability of aerosol penetration through respirator filters," *American Industrial Hygiene Association journal*, vol. 59, no. 7, pp. 461–465, 1998, ISSN: 0002-8894. DOI: 10.1080/15428119891010208. [Online]. Available: https://doi.org/10.1080/15428119891010208.

[16] N. Hasolli, Y. O. Park, and Y. W. Rhee, "Experimental study on filtration performance of flat sheet multiple-layer depth filter media for intake air filtration," *Aerosol Science and Technology*, vol. 47, no. 12, pp. 1334–1341, 2013. DOI: 10.1080/02786826.2013.842281. eprint: https://doi.org/10.1080/02786826.2013.842281. [Online]. Available: https://doi.org/10.1080/02786826.2013.842281.

[17] K. Sutherland, "Filtration overview: A closer look at depth filtration," *Filtration & Separation*, vol. 45, no. 8, pp. 25–28, 2008, ISSN: 0015-1882. DOI: https://doi.org/10.1016/S0015-1882(08)70296-9. [Online]. Available: https://www.sciencedirect.com/science/article/pii/S0015188208702969.

[18] A. Onur, A. Ng, W. Batchelor, and G. Garnier, "Multi-layer filters: Adsorption and filtration mechanisms for improved separation," *Frontiers in Chemistry*, vol. 6, p. 417, 2018, ISSN: 2296-2646. DOI: 10.3389/fchem.2018.00417. [Online]. Available: https://www.frontiersin.org/article/10.3389/fchem.2018.00417.

[19] TSI Incorporated, "Mechanisms of Filtration for High Efficiency Fibrous Filters - Application Note ITI-041," *TSI Incorporated.*, vol. 041, pp. 1–4, 2012. [Online]. Available: https://www.tsi.com/getmedia/4982cf03-ea99-4d0f-a660-42b24aedba14/ITI-041-A4?ext=.pdf.

[20] A. Tcharkhtchi, N. Abbasnezhad, M. Zarbini Seydani, N. Zirak, S. Farzaneh, and M. Shirinbayan, "An overview of filtration efficiency through the masks: Mechanisms of the aerosols penetration," *Bioactive Materials*, vol. 6, no. 1, pp. 106–122, 2021, ISSN: 2452-199X. DOI: https://doi.org/10.1016/j.bioactmat.2020.08.002. [Online]. Available: https://www.sciencedirect.com/science/article/pii/S2452199X20301481.

[21] D. Kalaivani, S. Karthick, and N. Gobi, "Filtration properties of staple fibre thermo-bonded nonwoven fabrics," 2016.

[22] C.-S. Wang, "Electrostatic forces in fibrous filters - a review," *Powder Technology*, vol. 118, no. 1, pp. 166–170, 2001, In Commemoration of Prof. Koichi Iinoya, edited by C. Kanaoka and H. Masuda, ISSN: 0032-5910. DOI: https://doi.org/10.1016/S0032-5910(01)00307-2. [Online]. Available: https://www.sciencedirect.com/science/article/pii/S0032591001003072.

[23] C. Wang, "Electrostatic forces in fibrous filter a review," *Powder Technology*, vol. 118, pp. 166–170, 2001.

[24] TSI, "Mechanisms of Filtration for High Efficiency Fibrous Filters," *TSI Inc.*, vol. 041, pp. 1–4, 2012.

[25] C. Yue, Q. Zhang, and Z. Zhai, "Numerical simulation of the filtration process in fibrous filters using cfd-dem method," *Journal of Aerosol Science*, vol. 101, pp. 174–187, 2016, ISSN: 0021-8502. DOI: https://doi.org/10.1016/j.jaerosci.2016.08.004. [Online]. Available: https://www.sciencedirect.com/science/article/pii/S0021850215301063.

[26] C. Yue, Q. Zhang, and Z. Zhai, "Numerical simulation of the filtration process in fibrous filters using CFD-DEM method," *J. Aerosol Sci.*, vol. 101, pp. 174–187, 2016, ISSN: 18791964. DOI: 10.1016/j.jaerosci.2016.08.004.

[27] D. Thomas, S. Pacault, A. Charvet, N. Bardin-Monnier, and J.-C. Appert-Collin, "Composite fibrous filters for nano-aerosol filtration: Pressure drop and efficiency model," *Separation and Purification Technology*, vol. 215, pp. 557–564, 2019, ISSN: 1383-5866. DOI: https://doi.org/10.1016/j.seppur.2019.01.043. [Online]. Available: https://www.sciencedirect.com/science/article/pii/S1383586618342643.

[28] N. Hasolli, Y. Park, and Y. Rhee, "Filtration performance evaluation of depth filter media cartridges as function of layer structure and pleat count," *Powder Technology*, vol. 237, pp. 24–31, 2013, ISSN: 0032-5910. DOI: https://doi.org/10.1016/j.powtec.2013.01.002. [Online]. Available: https://www.sciencedirect.com/science/article/pii/S0032591013000193.

[29] C. Davies, "Filtration of aerosols," *Journal of Aerosol Science*, vol. 14, no. 2, pp. 147–161, 1983, ISSN: 0021-8502. DOI: https://doi.org/10.1016/0021-8502(83)90039-3. [Online]. Available: https://www.sciencedirect.com/science/article/pii/0021850283900393.

[30] D. Thomas, P. Penicot, P. Contal, D. Leclerc, and J. Vendel, "Clogging of fibrous filters by solid aerosol particles experimental and modelling study," *Chemical Engineering Science*, vol. 56, no. 11, pp. 3549–3561, 2001, ISSN: 00092509. DOI: 10.1016/S0009-2509(01)00041-0.

[31] C. N. Davies, "The separation of airborne dust and particles," *Proceedings of the Institution of Mechanical Engineers*, vol. 167, no. 1b, pp. 185–213, 1953. DOI: 10.1177/002034835316701b13. eprint: https://doi.org/10.1177/002034835316701b13. [Online]. Available: https://doi.org/10.1177/002034835316701b13.

[32] W. C. Hinds, *Aerosol Technology : Properties, Behavior, and Measurement of Airborne Particles*. 1967, pp. 182–205. [Online]. Available: https://ebookcentral.proquest.com/lib/ualberta/detail.action?docID=1120423..

[33] R.C.Brown, *Air filtration: An integrated approach to the theory and applications of fibrous filters*. Oxford; New York: Pergamon Press, 1993. DOI: 10.1016/0021-8502(95)90072-1.

[34] H.-C. Yeh and B. Y. Liu, "Aerosol filtration by fibrous filters–i. theoretical," *Journal of Aerosol Science*, vol. 5, no. 2, pp. 191–204, 1974, ISSN: 0021-8502. DOI: https://doi.org/10.1016/0021-8502(74)90049-4. [Online]. Available: https://www.sciencedirect.com/science/article/pii/0021850274900494.

[35] K. W. Lee and B. Y. H. Liu, "Theoretical study of aerosol filtration by fibrous filters," *Aerosol Science and Technology*, vol. 1, no. 2, pp. 147–161, 1982. DOI: 10.1080/02786828208958584. eprint: https://doi.org/10.1080/02786828208958584. [Online]. Available: https://doi.org/10.1080/02786828208958584.

[36] C. YANG, "Aerosol filtration application using fibrous media an industrial perspective," *Chinese Journal of Chemical Engineering*, vol. 20, no. 1, pp. 1–9, 2012, ISSN: 1004-9541. DOI: https://doi.org/10.1016/S1004-9541(12)60356-5. [Online]. Available: https://www.sciencedirect.com/science/article/pii/S1004954112603565.

[37] C. Brochot, A. Bahloul, P. Abdolghader, and F. Haghighat, "Performance of mechanical filters used in general ventilation against nanoparticles," *IOP Conf. Ser. Mater. Sci. Eng.*, vol. 609, no. 3, 2019, ISSN: 1757899X. DOI: 10.1088/1757-899X/609/3/032044.

[38] J. C. Keith, C. H. and Derrick, "MEASUREMENT OF THE PARTICLE SIZE DISTRIBUTION CONCENTRATION OF CIGARETTE SMOKE BY THE " CONIFUGE "," *J. Colloid Sci.*, vol. 356, no. 15, pp. 340–356, 1960.

[39] R. Trevisi, F. Cardellini, F. Leonardi, C. Vargas Trassierra, and D. Franci, "Acomparison of radon and its decay products' behaviour in indoor air," *Radiat. Prot. Dosimetry*, vol. 162, no. 1-2, pp. 171–175, 2014, ISSN: 17423406. DOI: 10.1093/rpd/ncu253.

[40] L. Stabile, F. C. Fuoco, and G. Buonanno, "Characteristics of particles and black carbon emitted by combustion of incenses, candles and anti-mosquito products," *Build. Environ.*, vol. 56, pp. 184–191, 2012, ISSN: 03601323. DOI: 10.1016/j.buildenv.2012.03.005. [Online]. Available: http://dx.doi.org/10.1016/j.buildenv.2012.03.005.

[41] N. Klepeis and W. Nazaroff, "Characterizing Size-Specific ETS Particle Emissions," *Indoor Air 2002 Proc. 9th Int. Conf. Indoor Air Qual. Clim. Held Monterey, California, June 30-July 5, 2002*, no. 1, pp. 162–167, 2002.

[42] J. Pagels, A. Wierzbicka, E. Nilsson, C. Isaxon, A. Dahl, A. Gudmundsson, E. Swietlicki, and M. Bohgard, "Chemical composition and mass emission factors of candle smoke particles," *J. Aerosol Sci.*, vol. 40, no. 3, pp. 193–208, 2009, ISSN: 00218502. DOI: 10.1016/j.jaerosci.2008.10.005.

[43] K. M. Lee, Y. M. Jo, J. H. Lee, and J. A. Raper, "Assessment of surface and depth filters by filter quality," *Powder Technology*, vol. 185, no. 2, pp. 187–194, 2008, ISSN: 0032-5910. DOI: https://doi.org/10.1016/j.powtec.2007.10.013. [Online]. Available: https://www.sciencedirect.com/science/article/pii/S0032591007005219.

[44] S.-H. Huang, C.-W. Chen, Y.-M. Kuo, C.-Y. Lai, R. McKay, and C.-C. Chen, "Factors affecting filter penetration and quality factor of particulate respirators," *Aerosol and Air Quality Research*, vol. 13, no. 1, pp. 162–171, 2013. DOI: 10.4209/aaqr.2012.07.0179. [Online]. Available: https://doi.org/10.4209%2Faaqr.2012.07.0179.

[45] B. H. Park, M.-H. Lee, Y. M. Jo, and S. B. Kim, "Influence of pleat geometry on filter cleaning in ptfe/glass composite filter," *Journal of the Air & Waste Management Association*, vol. 62, no. 11, pp. 1257–1263, 2012. DOI: 10.1080/10962247.2012.696530. eprint: https://doi.org/10.1080/10962247.2012.696530. [Online]. Available: https://doi.org/10.1080/10962247.2012.696530.

[46] J. S. Russo and E. Khalifa, "Computational study of breathing methods for inhalation exposure," *HVAC R Res.*, vol. 17, no. 4, pp. 419–431, 2011, ISSN: 10789669. DOI: 10.1080/10789669.2011.578701.

[47] E. Koch, *MULTI-LAYER FILTER*, 1984.

[48] A. Onur, A. Ng, W. Batchelor, and G. Garnier, "Multi-Layer Filters: Adsorption and Filtration Mechanisms for Improved Separation," *Front. Chem.*, vol. 6, no. September, pp. 1–11, 2018, ISSN: 2296-2646. DOI: 10.3389/fchem.2018.00417.

[49] L. DU, X. CHEN, W. LI, and Q. ZHU, "A study on enhancement of filtration process with filter aids diatomaceous earth and wood pulp cellulose," *Chinese Journal of Chemical Engineering*, vol. 19, no. 5, pp. 792–798, 2011, ISSN: 1004-9541. DOI: https://doi.org/10.1016/S1004-9541(11)60058-X. [Online]. Available: https://www.sciencedirect.com/science/article/pii/S100495411160058X.

[50] P. A, "Improving Depth Filtration Capacity and Flux Constant Flow Filtration : Depth vs . Dynamic Depth," *Advanced Minerals Corporation*, pp. 1–4, 2016.

[51] M. M. Rahman, P. Ashwin, and I Thakkar, "Use of Nano Fibers in Filtration-A Review," *IJSRD-International J. Sci. Res. Dev.*, vol. 4, no. June, pp. 2321–0613, 2016. [Online]. Available: www.ijsrd.com.

[52] S. C. Kim, S. Kang, H. Lee, D.-B. Kwak, Q. Ou, C. Pei, and D. Y. Pui, "Nanofiber filter performance improvement: Nanofiber layer uniformity and branched nanofiber," *Aerosol and Air Quality Research*, vol. 20, no. 1, pp. 80–88, 2020. DOI: 10.4209/aaqr.2019.07.0343. [Online]. Available: https://doi.org/10.4209%2Faaqr.2019.07.0343.

[53] L. Sundstrom, A. Brolin, and N. Hartler, "Fibrillation and its importance for the properties of mechanical pulp fiber sheets," *Nord. Pulp Pap. Res. J.*, vol. 8, no. 4, pp. 379–383, 1993, ISSN: 0283-2631. DOI: 10.3183/npprj-1993-08-04-p379-383.

[54] S. Zhang, H. Liu, X. Yin, J. Yu, and B. Ding, "Anti-deformed Polyacrylonitrile/Polysulfone Composite Membrane with Binary Structures for Effective Air Filtration," *ACS Appl. Mater. Interfaces*, vol. 8, no. 12, pp. 8086–8095, 2016, ISSN: 19448252. DOI: 10.1021/acsami.6b00359.

[55] J. Liu, X. Zhang, H. Zhang, L. Zheng, C. Huang, H. Wu, R. Wang, and X. Jin, "Low resistance bicomponent spunbond materials for fresh air filtration with ultra-high dust holding capacity," *RSC Adv.*, vol. 7, no. 69, pp. 43 879–43 887, 2017, ISSN: 20462069. DOI: 10.1039/c7ra07694k.

[56] O. O. Fadare and E. D. Okoffo, "Covid-19 face masks: A potential source of microplastic fibers in the environment," *Sci. Total Environ.*, vol. 737, no. January, 2020.

[57] W. H. Seto, D. Tsang, R. W. Yung, T. Y. Ching, T. K. Ng, M. Ho, L. M. Ho, and J. S. Peiris, "Effectiveness of precautions against droplets and contact in prevention of nosocomial transmission of severe acute respiratory syndrome (SARS)," *Lancet*, vol. 361, no. 9368, pp. 1519–1520, 2003, ISSN: 01406736. DOI: 10.1016/S0140-6736(03)13168-6.

[58] J. Mao, B. Columbia, B. Grgic, W. H. Finlay, and J. F. Kadla, "Wood pulp based filters for removal of sub-micrometer," *Nord. Pulp Pap. Res. J.*, vol. 23, no. October 2017, pp. 2–8, 2008. DOI: 10.3183/NPPRJ-2008-23-04-p420-425.

[59] T. Obokata and A. Isogai, "The mechanism of wet-strength development of cellulose sheets prepared with polyamideamine-epichlorohydrin (pae) resin," *Colloids and Surfaces A: Physicochemical and Engineering Aspects*, vol. 302, no. 1, pp. 525–531, 2007, ISSN: 0927-7757. DOI: https://doi.org/10.1016/j.colsurfa.2007.03.025. [Online]. Available: https://www.sciencedirect.com/science/article/pii/S0927775707002361.

[60] J. Mao, J. F. Kadla, and R. J. Kerekes, "Retaining surface fibrillation of wet-beaten wood pulp in the dry state," *TAPPI J.*, no. july, pp. 25–30, 2009.

[61] U. F. Service, "Morphology Wood Pulp From Softwoods and Influence on Paper," *Agriculture*, 1974.

[62] A. L. MacFarlane, J. F. Kadla, and R. J. Kerekes, "High performance air filters produced from freeze-dried fibrillated wood pulp: Fiber network compression due to the freezing process," *Ind. Eng. Chem. Res.*, vol. 51, no. 32, pp. 10 702–10 711, 2012, ISSN: 08885885. DOI: 10.1021/ie301340q.

[63] K. P. Fennelly, "Particle sizes of infectious aerosols: implications for infection control," *Lancet Respir. Med.*, vol. 8, no. 9, pp. 914–924, 2020, ISSN: 22132619. DOI: 10.1016/S2213-2600(20)30323-4. [Online]. Available: http://dx.doi.org/10.1016/S2213-2600(20)30323-4.

[64] J. Dhivyadharshini, J. Somasundaram, and M. P. Brundha, "Composition and uses of N95 masks -a review," *European Journal of Molecular and Clinical Medicine*, vol. 7, no. 1, pp. 1529–1540, 2020, ISSN: 25158260.

[65] M. V. Lozano, M. J. Santander-Ortega, and M. J. Alonso, "Chapter 14 - in vitro relevant information for the assessment of nanoparticles for oral drug administration," in *Nanotechnology for Oral Drug Delivery*, J. P. Martins and H. A. Santos, Eds., Academic Press, 2020, pp. 419–458, ISBN: 978-0-12-818038-9. DOI: https://doi.org/10.1016/B978-0-12-818038-9.00014-4. [Online]. Available: https://www.sciencedirect.com/science/article/pii/B9780128180389000144.